DESIGN AND FABRICATION OF A RHOMBIC DRIVE STIRLING CYCLE CRYOGENIC REFRIGERATOR

Charles Balas, Jr.

Philips Laboratories

Prepared for:

Army Mobility Equipment Research and Development Center

July 1973

KEY WORDS	LINK A		LINK B		LINK C	
	ROLE	WT	ROLE	WT	ROLE	WT
cryogenic refrigerator						
cryogenics						
Stirling cycle						
rhombic drive						

DESIGN AND FABRICATION OF A RHOMBIC DRIVE STIRLING CYCLE CRYOGENIC REFRIGERATOR

Final Report

by

Charles Balas, Jr.

July 1973

Prepared for

U.S. Army Mobility Equipment Research & Development Center
Fort Belvoir, Virginia 22060

Contract No. DAAK02-72-C-0224

Prepared by

PHILIPS LABORATORIES
A Division of North American Philips Corporation
Briarcliff Manor, New York 10510

DOCUMENT CONTROL DATA - R & D

(Security classification of title, body of abstract and indexing annotation must be entered when the overall report is classified)

1. ORIGINATING ACTIVITY (Corporate author)	2a. REPORT SECURITY CLASSIFICATION
Philips Laboratories 345 Scarborough Road Briarcliff Manor, New York 10510	2b. GROUP

3. REPORT TITLE

Design and Fabrication of a Rhombic Drive Stirling Cycle Cryogenic Refrigerator

4. DESCRIPTIVE NOTES *(Type of report and inclusive dates)*

Final Report: 4 February 1972 to 29 June 1973

5. AUTHOR(S) *(First name, middle initial, last name)*

Charles Balas, Jr.

6. REPORT DATE	7a. TOTAL NO. OF PAGES	7b. NO. OF REFS
July 1973	~~X~~ 89	6

8a. CONTRACT OR GRANT NO	9a. ORIGINATOR'S REPORT NUMBER(S)
DAAK02-72-C-0224 b. PROJECT NO.	
c.	9b. OTHER REPORT NO(S) *(Any other numbers that may be assigned this report)*
d.	

10. DISTRIBUTION STATEMENT

DISTRIBUTION STATEMENT A
Approved for public release; Distribution Unlimited

11. SUPPLEMENTARY NOTES	12. SPONSORING MILITARY ACTIVITY
	USAMERDC Fort Belvoir, Virginia

13. ABSTRACT

The purpose of this program was to develop a quiet, vibration-free, long-life, lightweight Stirling cycle refrigerator capable of producing 1 W of cold at 77°K while in a still air environment at 125°F. The total power consumption of the machine was restricted to 42 W. To attain high efficiency, a double-expansion regenerator with a titanium alloy shell was utilized along with a titanium cold finger with copper cap. The balanced Philips rhombic drive provided the necessary drive motion without causing unwanted vibration. Brushless dc motors and dry lubrication throughout the refrigerator insured that contamination was minimized. A major acoustical study and design resulted in a variety of sound isolation techniques being applied. The refrigerator weighs 8 lbs. 7 oz., measures 5-7/8" x 5-5/16" x 9-1/4" and is inaudible at 63 ft. against a 40 dbA background. With the most disadvantageous heat exchanger orientation in still air at 125°F, cooldown time with a 0.5 W heat leak is 3-1/2 minutes and the refrigerator produces 1.06 W of cold at 80°K with a shaft power input of only 25.6 W. As a result of inefficient drive motors, the unit consumes more than 42 W and does not function properly in the -65°F ambient. With the exception of the motor shortcomings, the refrigerator meets all required specifications.

DD FORM 1 NOV 1473 REPLACES DD FORM 1473, 1 JAN 64, WHICH IS OBSOLETE FOR ARMY USE.

Unclassified

Security Classification

SUMMARY

The purpose of this program was to develop a quiet, vibration-free, long-life, lightweight Stirling cycle refrigerator capable of producing one (1) watt of cold at 77°K while in a still air environment at 125°F. The total power consumption of the machine was restricted to 42 watts. To attain high efficiency, a double-expansion regenerator with a titanium alloy shell was utilized along with a titanium cold finger with copper cap. The balanced Philips rhombic drive provided the necessary drive motion without causing unwanted vibration. Brushless dc motors and dry lubrication throughout the refrigerator insured that contamination was minimized. A major acoustical study and design resulted in a variety of sound isolation techniques being applied.

The refrigerator weighs 8 lbs. 7 oz., measures 5-7/8" x 5-5/16" x 9-1/4" and is inaudible at 63 feet against a 40 dbA background. With the most disadvantageous heat exchanger orientation in still air at 125°F, cooldown time with a 0.5 watt heat leak was 3-1/2 minutes and the refrigerator produced 1.06 watts of cold at 80°K with a shaft power input of only 25.6 watts. The brushless dc drive motor proved to be below specification in efficiency and was unable to produce the torque required for refrigerator operation in a -65°F ambient. As a consequence, the unit consumed more than 42 watts of power and did not function properly in the -65°F ambient.

In summary, with the exception of the drive motor shortcomings, the refrigerator meets all required specifications. Presently, the option exists to replace these motors with available 65% efficient brush-type motors, or in the future to replace them with more efficient brushless motors.

FOREWORD

The work described in this report was performed at Philips Laboratories, a Division of North American Philips Corporation, Briarcliff Manor, New York, under the supervision of Mr. Alexander Daniels, Director, Mechanical Systems Research Group. The project engineer was Charles Balas, Jr. Dr. Frits K. du Pré, Consulting Scientist of Philips Laboratories, provided analytical assistance. Dr. Richard C. Sweet, Supervisor, Heat Processing Laboratory, was instrumental in the dewar and cold finger fabrication; and Mr. Bruno Smits, Chief Designer, aided in the hardware design. Assisting in the investigation of the acoustical noise problems associated with the refrigerator design was Mr. Lewis Bell of Harold Mull, Bell and Associates. Fabrication was supervised by Mr. George Potanovic, Assistant Foreman of the Instrument Shop. Technician Richard Petendree performed the refrigerator tests and assisted in developing the refrigerator.

This program was issued by the U. S. Army Mobility Equipment Research and Development Center, Fort Belvoir, Virginia, and was initiated under Contract DAAK02-72-C-0224. Mr. Stuart Horn was the Contracting Officer's Representative for the Night Vision Laboratory, USAECOM.

The work described in this Final Report covers the period from 4 February 1972 to 29 June 1973.

TABLE OF CONTENTS

LIST OF ILLUSTRATIONS

1. INTRODUCTION

1.1 Objectives

The goal of this program was to design, fabricate, test and evaluate a low-noise, low-power rhombic drive Stirling cycle cooler with the following performance specifications:

Life:	3000 hours with purging intervals every 500 hours (2000 hour design goal).
Weight:	8.5 lbs maximum (with a goal of 6 lbs) for the cooler proper plus an additional 3.5 lbs maximum for inverters.
Acoustic Noise:	While being rigidly mounted to an aluminum plate of dimensions 2' x 2' x 1/2", the cooler shall be inaudible to a human operator at a distance of 100 ft, against a background level of 40 dbA above the reference level rms sound pressure of 2.04×10^{-4} dyne per cm^2. As a design goal the cooler should be inaudible at a distance of 25 ft against this background.
Cooldown Time:	5 min with a goal of 3 min or less to reach 77°K with a simulated thermal heat leak equivalent to 1/2 W at 77°K in a 125°F ambient.

Environmental Operation Range:	-65°F to 125°F and altitudes up to 5000 ft.
Operating Temperature:	77°K ± 5°K in the 125°F ambient
Output Refrigeration:	1 W at 77°K
Input Power:	42 W max
Mechanical Vibration:	Cold finger displacements less than 0.0002" peak-to-peak and 0.00002" peak-to-peak along and perpendicular to the cold finger axes, respectively.
Operating Modes:	Any orientation, and up to 5 g acceleration.
Size:	5-5/8" x 7-1/4" x 10" with a goal of 5" x 6" x 8".

1.2 Background

The Stirling cycle is well known as a means of producing refrigeration at cryogenic temperatures. The high thermodynamic efficiencies attained with this cycle have made it desirable for many applications. Efforts to significantly improve the operating characteristics of the Stirling refrigerator without forfeiting its low weight and high efficiency were initiated with this project. The basic theory of both the theoretical and actual Stirling cycle is presented in Appendix A. Other Philips advances incorporated in the refrigerator, viz., the efficient double-expansion process and the vibration-free rhombic drive, are described in Appendices B and C, respectively.

1.3 Approach to the Problem

The basic approach to the design of this refrigerator was twofold: thermodynamic and mechanical analytical studies were made to optimize all parameters; an existing rhombic-drive, Stirling cycle refrigerator (Cryogem®) was used as a model and test machine for evaluating design changes.

Major design trade-offs that were considered are:

- The weight of the machine envelope versus acoustical noise.
- Refrigerator life versus power consumption which is a function of bearing and seal design.
- Vibration of the cold finger due to the cyclic pressure variation of the working gas versus heat transfer losses due to conduction along the cold finger and versus charge

pressure which influences both cycle efficiency and bearing loads which in turn influence bearing life.

- Cooldown time and net refrigeration produced versus design variables such as charge pressure; pressure ratio; displacer stroke; mass and specific heat of the cold parts; overall structure of the regenerator, heat exchanger, and cold finger; and overall efficiency of the machine.

In addition, the following critical design areas were investigated:

- Acoustical noise. In-house design and testing, aided by an outside consultant, was used to reduce the noise production well below required levels.

- Efficiency. All components of the refrigerator were analyzed so as to optimize overall efficiency.

- Life and reliability. Performance and failure data from the existing Cryogem refrigerator were reviewed. Components that had previously failed or were suspected of having caused failures were redesigned.

- Weight and size. Lightweight alloys and compact efficient motors were selected. An effort was made to not jeopardize the low-noise-level of the machine.

- Refrigeration and cooldown time. Reduce friction losses; increase thermodynamic efficiency; minimize the heat capacity of cold parts without allowing significant pressure-induced vibration of the cold finger; increase

gas pressure and pressure ratio without again causing cold finger vibration and other system losses.

2. INVESTIGATION

2.1 Design and Test Effort

2.1.1 Acoustical Noise

An existing rhombic-drive, Stirling cycle refrigerator (a miniaturized Cryogem) was used as a test vehicle for the acoustical design of the final refrigerator. It was tested and modified with the purpose of determining as many ways as possible to reduce the total noise production in this unit and, of course, in the final design.

(1) Modification to Cryogem and Initial Test Results

Investigations revealed specific areas where generation and/or transmission of vibrations and acoustical noise were occuring:

Clearance and play in bearings. The majority of the bearings in the rhombic drive were made of Rulon. This type of bearing, however, allowed axial and radial movement of the drive mechanism, which in time resulted in excessive wear and motion. Teflon spacers were fitted between all metal drive parts that might make contact; both new Rulon bearings and replacement roller-type bearings were tried. All changes resulted in lower noise levels. A reduction in noise level was difficult to measure since these tests were performed in an environment having a varying noise level; the variation in background noise was the same order of magnitude as the noise reductions.

Metal-to-metal contact. In addition to the above, the displacer rod which connects the lower rhombic yoke to the displacer wore through the piston displacer rod seal and made contact with the metal piston. The cause was due to:

unparallel yokes in the drive resulting from uneven torques delivered by the drive motors, excess play in the bearings and timing gears, and too many degrees of freedom in the displacer rod motion. There was also a metallic-noise transmission path through the shaft bearings into the crankcase. Possible solutions to this problem were not easy to test; therefore, their investigation was restricted to the design phase of the new refrigerator.

Gear noise. The timing gears connecting the two drive shafts were made of different materials to reduce tooth-generated noise. Two blends of Delrin were used, but the amount of noise reduction could not be accurately detected.

Thin walled sections. The cylindrical aluminum motor housings on the test cooler were 0.156 inch thick, and substantially more noise emanated from these walls than from the 0.25 to 0.50 inch thick crankcase. A laminate of urethane foam and lead sheet was added to part of the motor housings, and a noise reduction was detected. A more complete addition of this laminate, equivalent to a 2 lb/ft^2 mass increase, was one of the major changes that resulted in the low noise levels shown by the lower curve in Figure 1. An unmounted or freely suspended Cryogem with this added mass yielded a similar curve. All the data shown in Figure 1 was taken with a General Radio Type 1558-A Octave-Band Noise Analyzer with a 1560-P6 microphone assembly and a Hewlett Packard Real-Time Audio Analyzer, model 8054A.

Heat exchanger fin noise. The fins of the small heat exchanger on the Cryogem were found to resonate, thereby generating noise. The added mass simulation previously mentioned reduced the noise level but it was found that properly placed damping material or

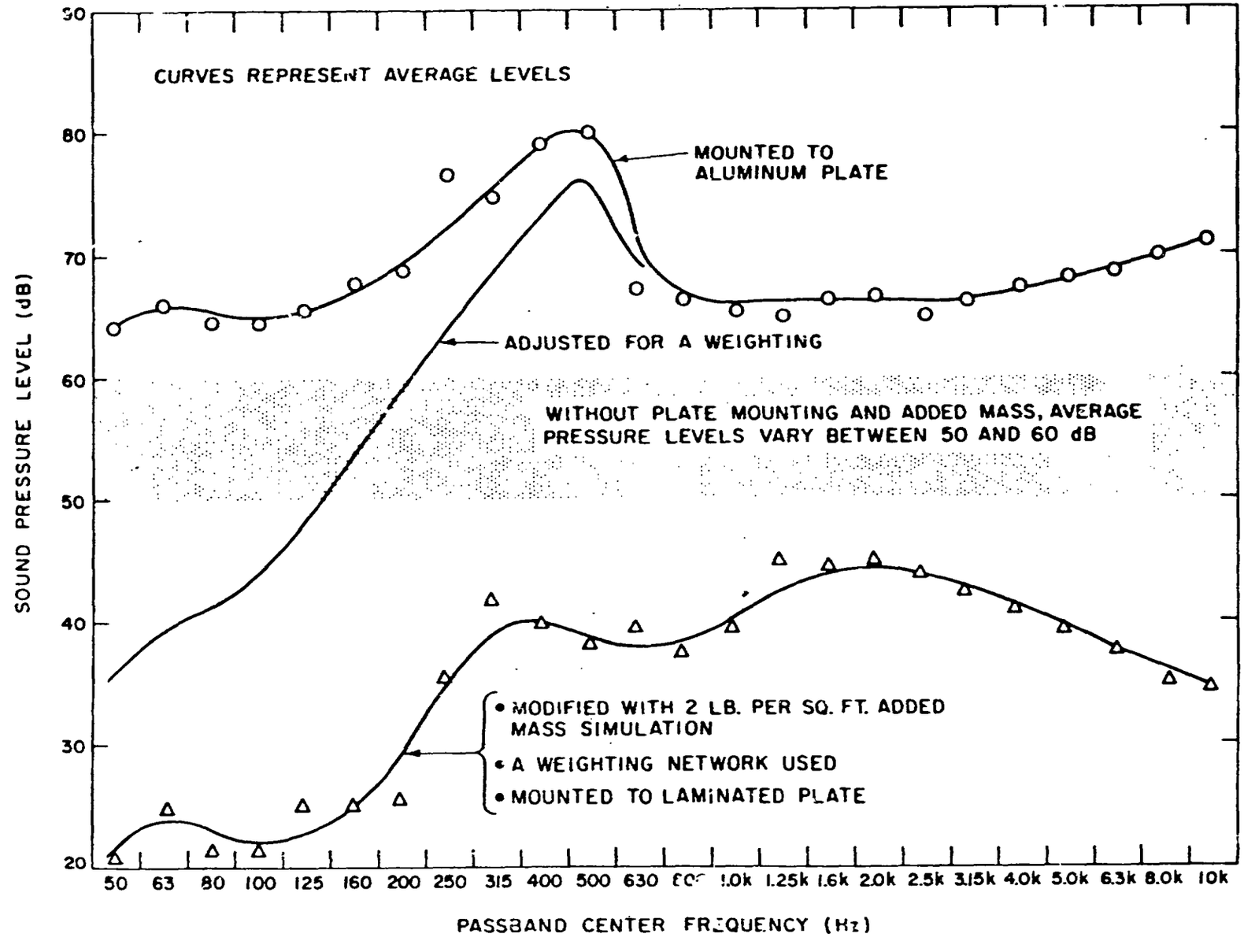

Figure 1: Average Sound Pressure Levels at One-Foot Distance and at Various Passband Center Frequencies for Rhombic Drive Cryogem Refrigerator (12 lb total wt)

fin-stiffening members also reduced the noise level as well, without seriously impeding heat transfer capability or adding significant weight.

Vibration and noise transmission. Pressure-induced strains on the refrigerator envelope, internally generated acoustical noise transmitted to this envelope, and small vibrations (due to the limit as to how well a theoretically perfect balance can be implemented) all add to the total noise production of the machine. Tests were performed to study the effects of noise and vibration transmitted to the refrigerator mounting plate. As seen in the uppermost curve in Figure 1, when the Cryogem was rigidly attached to an aluminum plate (24" x 24" x 1/2"), the acoustical noise level of the entire assembly became exceedingly high. This was so because the plate, in addition to radiating transmitted noise, vibrated and produced even more noise. The straightforward solution to this problem would be to isolate the refrigerator from the plate using vibration mounts or appropriate elastic materials. This, however, was not acceptable since the refrigerator, to be useful in an optical system, must be rigidly fixed to the plate. A laminated plate composed of alternate layers of 1/16" thick aluminum and CP-2-LC damping material manufactured by the Soundcoat Co., Inc. proved to be an acoustically acceptable mounting plate for the refrigerator. The overall dimensions of this fabricated plate were the required 24" square by 1/2", and with the Cryogem rigidly mounted to it there was almost no increase in transmitted and induced noise. Even when lengths of aluminum angle brackets were bolted to the underside of the laminated plate to increase its stiffness to that of the solid aluminum plate, no increase in noise level could be detected. In fact, the frequency distribution of the

sound pressure level measured for the cooler mounted to this laminated plate was essentially the same as that obtained from a freely suspended cooler.

As mentioned, the upper curve in Figure 1 represents the extreme case of the Cryogem rigidly mounted to the aluminum plate. Also shown is the effect of adjusting the sound pressure levels at the various frequencies using the A weighting scale. This closely approximates the response of the human ear, and since one of the program objectives is to develop a refrigerator that is inaudible to humans at specific distances, the A scale was used to weigh all sound pressure levels.

Eliminating from further consideration the aluminum plate-mounted system because of its high noise level, and the system utilizing added envelope mass (shown as the lowest curve in Figure 1) because of its high total weight, a more realistic refrigerator system was studied. The variation of sound pressure level with frequency of such a system is depicted as the center band in Figure 1. This represents the average acoustical spectrum of the freely suspended (or laminated plate-mounted) Cryogem without added mass. For measuring the overall sound pressure level of this refrigerator, the A scale of a General Radio type 1551-C sound-level meter with a GR type 1560-P5 microphone was used. It indicated a total of 67 dbA for the noise level three feet from a freely floating or laminated plate-mounted Cryogem refrigerator. At a distance of three feet from the refrigerator, no significant directionality of the sound pressure level could be detected.

Thus, points three feet from the refrigerator are in the far field, where the sound pressure level decreases 6 db for each doubling of distance. The noise level at three feet could be used to conservatively determine how the noise will be attenuated. The following equation (Ref. 1) will be used to determine the sound pressure level, L_p, in decibels at a distance r when the sound pressure level L_x at a distance r_x is known:

$$L_p = L_x - 20 \log_{10} \frac{r}{r_x}$$

Implicit in this equation is the assumption of a free sound field which is in a homogeneous isotropic medium free from boundaries. Since the noise source may be on the ground, 3 db will be added to the above expression (as is shown in Ref. 1) to account for ground reflection:

$$L_p = L_x - 20 \log_{10} \frac{r}{r_x} + 3$$

For $r = 100$ ft and $r_x = 3$ ft,

$$L_p = L_x - 20 \log_{10} \frac{100}{3} + 3$$

$$L_p = L_x - 30.5 + 3$$

$$L_p = L_x - 27.5 \text{ db}$$

For $L_x = 67$ dbA,

$$L_p = 67 - 27.5$$

$$L_p = 39.5 \text{ dbA}$$

This indicates that with a background level of 40 dbA the existing modified refrigerator would most likely be inaudible to a human observer. The situation is marginal since the major frequencies of the machine-generated noise and of the background noise could be significantly different, thereby making the refrigerator audible.

It should be noted, however, that the above analysis is conservative since it neglects any excess attenuation. A similar but more realistic analysis of the same problem is presented in Chapter 9 of Reference 2. Here excess attenuation terms which would result in a reduced value of L_p are included. Although these terms will not be incorporated into this analysis, they will be mentioned because in any realistic application some of them will be quite significant. They include attenuation due to atmospheric turbulence, wind, temperature gradients, ground effects (since ground in general will not behave as the perfect reflector assumed in the derivation of the formula used above), walls, trees, fog, rain, snow and absorption in air.

Magnesium was used for the crankcase walls because it has high internal damping and can be relatively thick since it is lightweight. The outer envelope panels were made as massive as possible, and are small to reduce the efficiency of low frequency sound radiation. Curvature and discrete bend lines were incorporated in the design of the outer envelope to raise the natural frequency of the panels and thereby reduce wave coincidence and resonance.

Noise level as a function of refrigerator operating speed will be measured to determine any resonances; if present, they will be reduced by adding damping material to the vibrating panels. Wave coincidence should not be a problem since all the crank-

case walls are thin enough to have natural frequencies greater than 1 kHz. However, if either wave coincidence or reverbration appear as problems, porous polyurethane liners will be added inside the crankcase to absorb sound energy, and if the resulting noise level is still too high, the offending panels will be damped.

In addition to pressure-induced envelope vibrations, the moving elements in the final refrigerator will generate impact, rolling and sliding noise and vibration. The magnitude of this noise and vibration will be at a practical minimum level as a result of the acoustical design, and some of it will be absorbed and isolated by the refrigerator envelope. But since this vibration and noise is the source of all other induced vibration, and since the transmission of all these disturbances to the refrigerator surroundings determines the overall acoustical noise level, an effort will be made to isolate this source from the rest of the machine. Metal-to-metal contact between moving and stationary parts will be eliminated by the teflon piston rings and displacer seals, the polyimide displacer rod bearings and seals, and the Kel-F bearing mounts. Thus, the impedance of the noise and vibration transmission path will be increased.

The basic concept being applied in varying the materials along the transmission path is that of constrained-layer damping. In this process, two materials of different stiffness vibrate out of phase, causing a shearing action in the less stiff layer. Energy absorption in this layer is due mainly to shear stress developed.

The same principle was used to deaden the gears and the refrigerator mounting plate. A laminate of aluminum and damping material was fabricated for the plate, and two blends of Delrin(®) with titanium-magnesium hubs were used for the gears.

Similarly the heat exchanger fins were experimentally quieted by placing spacers between them at optimum points.

(2) Final Acoustical Design

The basic approach to the final refrigerator design was to reduce the generation of acoustic noise and mechanical vibration as much as possible and to absorb and isolate as much of the remaining sound and vibration as practical within the project constraints. It was therefore decided to design as quiet a refrigerator as possible utilizing free-convection heat rejection. If forced convection cooling were used, the blower could be small and of acceptable weight but to be reasonably efficient it would have to operate at a high noise-producing speed. This additional noise would necessitate an acoustic enclosure, only adding to the total weight and size of the refrigerator. Alternatively, a low speed blower could have been used, but the high power consumption, physical size and weight of such a unit made it unattractive. Therefore, considering the project objectives, a free convection cooled unit with inherent low-noise generation appeared to be the more reasonable choice over a forced convection cooled unit with either its high weight, size and power consumption or its higher noise levels being absorbed and isolated by an additional acoustic container. These high noise levels would be from both the fan-generated noise and the additional refrigerator noise transmitted through the thinner refrigerator envelope walls; the walls being thinner to partially

compensate for the greater mass of the acoustical barrier material. Barrier materials, to make effective enclosures, must have a low specific stiffness, like lead for example.

Continuing with the first approach in the acoustical design, viz., to reduce the generation of acoustic noise and mechanical vibration as much as possible, the following approaches were employed in the final refrigerator design:

Low value of moving mass. Aside from overall weight considerations, reducing the magnitude of reciprocating and even rotating mass will reduce bearing loads, wear and resulting noise.

High precision in drive mechanism. Improving alignment and reducing tolerances and clearances will reduce wear and impact noise, especially in the two gears and in the rhombic drive. Also, teflon spacers will be fitted between all moving parts in the rhombic drive to prevent metal-to-metal contact.

Optimum bearings. Radial ball bearings will be used exclusively in the rhombic drive. Even though they produce acoustical noise, it is of relatively high frequency which is more readily attenuated than low frequency noise. In previous tests, the noise from the ball bearings was more evenly distributed than the impact noise generated with sleeve type bearings. Also, the ball bearings exhibited less wear than the sleeve type bearings. This should result in less noise increase with time.

Low friction materials. In addition to bearing wear, there are other acoustically critical wear areas. These include seals and guides fabricated from Rulon™ when loading is low or areas are large, and from Feuralon™ AW, a silver and tungsten disulfide

filled polyimide, when loading is high or areas are small. So minimum noise producing wear will be achieved with minimum friction. (The problem of wear is considered in more detail in Par. 2.1.2.).

Low operating speed. A low speed machine is desirable because, in general, as the speed is reduced so is the generated noise. However, 1500 rpm was selected as a compromise speed since at lower speeds the D.C. motor would become less efficient or gearing would be needed with more efficient higher speed motors. Sealing would also become a problem at low speeds, necessitating high friction, high wear seals or allowing substantial gas blowby with low friction seals. Low speeds would also require high charge pressures leading to increased bearing loads and associated higher noise levels, weight, size and power consumption.

Precision balance. Either static or dynamic unbalance eventually result in additional acoustical noise. It is therefore important to implement as well as possible the theoretically perfect balance of the rhombic drive.

Large buffer volume. The larger the volume of gas in the crankcase, the less the pressure variation due to displacer rod and piston motion, and the lower the stress on the crankcase envelope. With the given crankcase, the gas volume is as large as possible so the resulting pressure induced envelope strains and vibrations are small.

The final considerations in the acoustical design of the refrigerator were to absorb and isolate as much of the remaining generated noise and vibration as practical. Included with this was an effort to prevent any additional resonance from being cited.

For very low frequencies, a panel must be stiff and thick for the transmission loss (i.e., the reduction of sound energy in transmission through a material), to be high. At moderate frequencies, panel mass is more critical. In general these regions are not well defined and a considerable amount of overlap exists, so the control of transmission loss is assumed by both mass and stiffness. (The Cryogem tests revealed that by adding mass to the refrigerator, lower overall noise levels resulted.) As even higher frequencies are considered, transmission loss is greater for high frequency waves. Therefore, as mentioned previously, ball bearings producing higher frequency noise are more desirable than plastic sleeve bearings producing low frequency noise. However, it should also be noted that wave coincidence can occur above the critical frequency of the panel. Resonance also can occur between the stiffness and mass controlled region. So to achieve the maximum transmission loss while keeping within the constraints imposed by the project objectives, a compromise was made as to the total mass of the panels.

2.1.2 Life and Reliability

The decision to use free-convection heat rejection, dry lubrication, and brushless motors was directly related to life and reliability. The heat rejection question was already discussed in Par. 2.1.1; of additional interest here is that the refrigerator reliability will be higher without a blower. An oil lubricated machine will, in general, have a longer life with a higher reliability, but at the cost of additional power consumption, added system complexity, and the added weight of lubricant and associated equipment (Refs. 3, 4). Considering the weight and power requirements, it was decided to redesign the dry lubricated drive of the Cryogem so as to achieve a life of 3,000 hours.

Other test data from the Cryogem refrigerator was reviewed to find all life-limiting areas. Failures had occurred in the Rulon A bearings, the nylon and Delrin gears, and the steel displacer rod. Problem areas were brush wear and contamination from wear debris and outgassed vapors.

Bearings. The results of a study of dry lubricated bearings for extended-life application are presented in References 5 and 6. This study was used as a guide in selecting the bearings for the drive mechanism. Plastic journal bearings of the type used in the Cryogem were not considered for this application since they have not exhibited an extended life nor can accurate life prediction be made for the impact type loading they experience after initial wear. Ball bearings were selected for all rotating elements because of their low-power consumption and high reliability. Peak loads for each bearing were calculated using a dynamic force analysis of the rhombic drive.

Then, each bearing was selected so the contact stresses resulting from these peak loads were less than the 125,000 psi value set by bearing manufacturers for extended-life applications of dry lubricated bearings. Feuralon™ AW (Bemol Corp.) was selected for the bearing retainer material because it has shown the lowest wear rate for high loading, and because its coefficient of friction is relatively low at the high temperatures which will occur in the bearings. Its film strength (that of a polyimide) is also greater than that of a Teflon base material, which is most often used in these applications. This is of importance since it is the transfer of this film from the retainer to the balls and races by which lubrication takes place. It is the stress resulting from high loading which will cause excessive wear if this stress is greater than the film strength of the transfer film. In fact, if this high stress situation occurs, large pieces of wear debris will be created and cause even higher stress risers in the path of the balls. Failure of the bearing will normally occur when the retainer is eventually worn away.

Brushless dc motors. The brush-type dc motors used in the Cryogem refrigerator were synchronized by the timing gears connecting them. Since these motors did not produce the same torque, the gears were heavily loaded and some failures occurred. Also, the displacer rod did not exhibit pure reciprocating motion; this led to bushing failures and displacer rod damage. These problems were solved by fabricating more accurate drive components, by aligning the drive more accurately, by using a more rigid displacer rod and constraining it at both ends so only linear motion was possible, and by using brushless dc drive motors. These two motors are con-

trolled by one electronic package and, as a consequence, cog or step simultaneously. Thus, the loading on the timing gears and on the displacer rod is greatly reduced.

Dynamic seals. Two seals are required for the double expansion regenerator, and Rulon A sleeve-type seals will be used for both. Both seals are about 0.009" thick and are bonded to the regenerator shell with epoxy. This type of seal has the advantages of being low in friction and wear debris production while maintaining an adequate seal for the 3,000 hour life. Results from a test apparatus (Ref. 4) that simulates the low pressure difference across the seals and that has a similar flexible rod that allows the regenerator to center itself in the cold finger sleeve show that these seals will certainly last the required time.

Feuralon AW, a silver and tungsten disulfide-filled polyimide, was used for the piston/displacer rod seal. Unlike Teflon base materials, the coefficient of thermal expansion of Feuralon AW is approximately that of the metals used for the piston and displacer rod, thereby reducing the problems of binding and excessive blow-by as the temperature varies.

As concluded in References 5 and 6, a glass-loaded Teflon Bal seal with a light spring expander appears optimum for the piston-to-cylinder seal. The optimization is with respect to sealing, wear, and friction. Molybdenum disulfide is also included with the glass filler to keep the friction as low as possible without sacrificing the glass wear resisting properties.

Helium Retention. From Reference 5 and Parker Seal Company's Engineering Report No. 08-135 (July 1968) and Technical Bulletin No. 66 (January 1970) and in-house data, it was concluded that neoprene O-rings with a 50% squeeze would be used for maximum helium retention. Leakage rates of approximately 1×10^{-7} std cc per sec cm are expected.

Contamination. The internally generated contamination has been minimized by using thin, long-wearing seals, dry lubrication, and brushless motors. A thorough vacuum bake-out will be performed and only high purity helium will be used.

2.2 Performance

2.2.1 Test Equipment

The test equipment used to evaluate the performance of the refrigerator was as follows:

Instrument	Manufacturer
Motor Power Supply	Harrison Labs. - Model #520A
Heater Load Power Supply	Hewlett Packard - #6217A
Vacuum Station	Veeco Vacuum Station - #V5-9
Thermocouples (Copper-Constantan)	Omega
Ice Point Reference	Kaye Inst. - #K 150-6C
Millivolt Potentiometer	Leeds & Northrup - #8686
Environmental Test Chamber	Tenney Engineering, Inc.
Sound Level Meter	General Radio Company - #1551-C
Wave Analyzer	General Radio Company - #1900A
Recording Wave Analyzer	General Radio Company - #1910A
Stop Watch	Minerva Company
Digital Multimeter	Keithley Company - #160
Voltmeter	Weston Inst. Inc. - Model #931
Absorption Dynamometer	John Chatillon & Sons - #2200
Oscilloscope	Tektronic, Inc. - Type 564B storage with Type 3A3 amplifier and Type 3B4 time base
Pressure Transducer	Kulite Semiconductor Prod. Inc. #XTL-140-200
Elapsed Time Meter	Curtis Inst. Inc. - Model #420LA
Leak Detector	Veeco - #MS-90

2.2.2 Cold Production

Testing the refrigerator at various charge pressures and in an ambient of 77°F yielded the following results: With a charge pressure of 78 psig, cold production was 0.792 watt at 77.5°K. By raising the charge pressure to 92 psig, a 1 watt load can be maintained at a temperature of 78°K with 23.4 watts of shaft power. Increasing the charge pressure to 100 psig allows the unit to except a 1.1 watt load at 78°K with 24 watts of shaft power. Low temperature tests were obtained by starting the

unit at 70°F and then gradually lowering the temperature of the environmental test chamber. With a 1.06 watt load, the refrigerator maintained 75°K at a -50°F ambient with 25 watts of shaft power. Lowering the ambient below -50°F caused a very erratic current drain. At the 125°F ambient (in still air), the unit required 25.6 watts of shaft power and maintained 80°F with a 1.06 watt load. These and other performance results are given in Tables 1 and 2.

Other pertinent performance results are as follows:

Conduction along thermocouple and heater leads: 0.016 watt. Vacuum in test dewar: minimum of 10^{-4} torr. Compression ratio: 1.7 to 1.8 was maximum obtained using one Bal seal with light spring expander which resulted in minimum friction losses. Clearance between regenerator stages and cold finger steps: 0.001" to 0.003" at T.D.C. (top dead center).

2.2.3 Cooldown

The cooldown requirements were met with no difficulty. At a 125°F ambient and with a 0.019" O.D. by 1.48" long copper wire installed in the cold finger to simulate a 0.5 watt heat leak, the unit cooled down to 77°K in 3.5 minutes with a shaft power of 23.5 watts. These tests were performed with a charge pressure of 100 psig and at a speed of 1500 rpm.

2.2.4 Acoustic Noise

Acoustic noise data was taken in a room approximately 25' x 25' x 10' with a 42 dbA ambient. Using a General Radio Sound Level Meter with a type 1560-P5 microphone, measurements were taken at various orientations at distances of 3 feet with the

Table 1
Refrigerator Performance Data:
Cooldown and Cold Production

PERTINENT COOL DOWN AND COLD PRODUCTION DATA

AMBIENT 70°F
CHARGE PRESSURE 100 psig

PRESSURE RATIO 1.8
SPEED 1500 RPM

TIME (MIN)	°K	P IN (WATTS)	P (SHAFT, WATTS)	LOAD (WATTS)	HEAT REJECTION TEMP °F (CRANKCASE)
2	82	47.78	20.5	0	70
5	43	60.51	26.9	0	73
25	78	53.17	23.7	1.1	85
	AMBIENT 125°F CHARGE PRESSURE 100 psig				
2	84	48.59	21.66	0	125
5	43	61.12	27.26	0	127
60	80	57.35	25.60	1.06	156

Table 1
Refrigerator Performance Data:
Cooldown and Cold Production

PERTINENT COOL DOWN AND COLD PRODUCTION DATA

AMBIENT 25°F — PRESSURE RATIO 1.78
CHARGE PRESSURE 92 psig — SPEED 1500 RPM

TIME (MIN)	°K	P IN (WATTS)	P (SHAFT, WATTS)	LOAD (WATTS)	HEAT REJECTION TEMP. °F (CRANKCASE)
2	73	59.7	26.5	0	25
5	39	67.0	30.0	0	28
25	76	61.0	26.0	1.03	50
50	76	60.0	26.8	1.04	50
AMBIENT-START AT 70°F THEN LOWER TO −50°F CHARGE PRESSURE 100 psig					PRESSURE RATIO 1.75 SPEED 1500 RPM
4	47	59.72	26.6	0	—
		AMBIENT 0°F			
24	76	54.9	24.4	1.06	44
		AMBIENT −40°F			
42	75	56	24.9	1.06	34
		AMBIENT −50°F			
50	75	62.54	27.89	1.06	26

Refrigerator Performance Data: Steady State
Cold Production at Various Heat Loads

STEADY STATE COLD PRODUCTION AT VARIOUS LOADS

125°F AMBIENT

	RUN I	RUN II	RUN III	RUN IV	RUN V
CHARGE PRESSURE (P.S.I.G.)	90	90	90	90	90
LOAD (WATTS)	1.02	0.75	0.50	.25	0
TEMPERATURE (°K)	81	70	62	49	43
TOTAL POWER IN (WATTS)	52.4	55.9	59.0	66.5	70
SHAFT POWER (WATTS)	23.4 → 25	24.9 → 25.5	26.3	29.7	31

25°F AMBIENT

CHARGE PRESSURE (P.S.I.G.)	85	85	85	85	85
LOAD (WATTS)	1.03	.75	.5	.25	0
TEMPERATURE (°K)	76	65	48	45	40
TOTAL POWER IN (WATTS)	58.3	62.2	64.3	67.8	68
SHAFT POWER (WATTS)	26.2	27.8	28.8	30.3	30.4

unit mounted on the 2' x 2' x 1/2" laminated plate. The formulas of Paragraph 2.1.1 were then applied. Figure 2 shows the sound pressure level associated with the refrigerator at various orientations and at distances of 3', 25', 50', 75' and 100'. These calculated values are conservative as mentioned in Paragraph 2.1.1. Slightly lower readings are obtained when the unit is freely suspended as opposed to plate mounted. Some dampening was employed on the mounting plate, such as the teflon heat exchanger fin dampener and the yellow dampening material that breaks the metal-to-metal contact between the refrigerator and the mounting plate. Figure 3 gives distances at various orientations around the plate-mounted refrigerator where one would have to stand for it to be marginally audible against a 40 dbA background. Figure 4 is a plot of relative response in db aginst frequency. In this particular test, the sound level meter was set on the C scale so that all frequencies were accepted. This signal was then passed through a General Radio Wave Analyzer. As seen from the plot, dominant frequencies appear at 450 Hz, 1.5 kHz, 2.75 kHz and 3.25 kHz. The signal representing ambient background frequencies was subtracted from the refrigerator signal so that a plot of the unit's relative response would be independent of the background noise. The refrigerator was plate-mounted as in previous noise measurements.

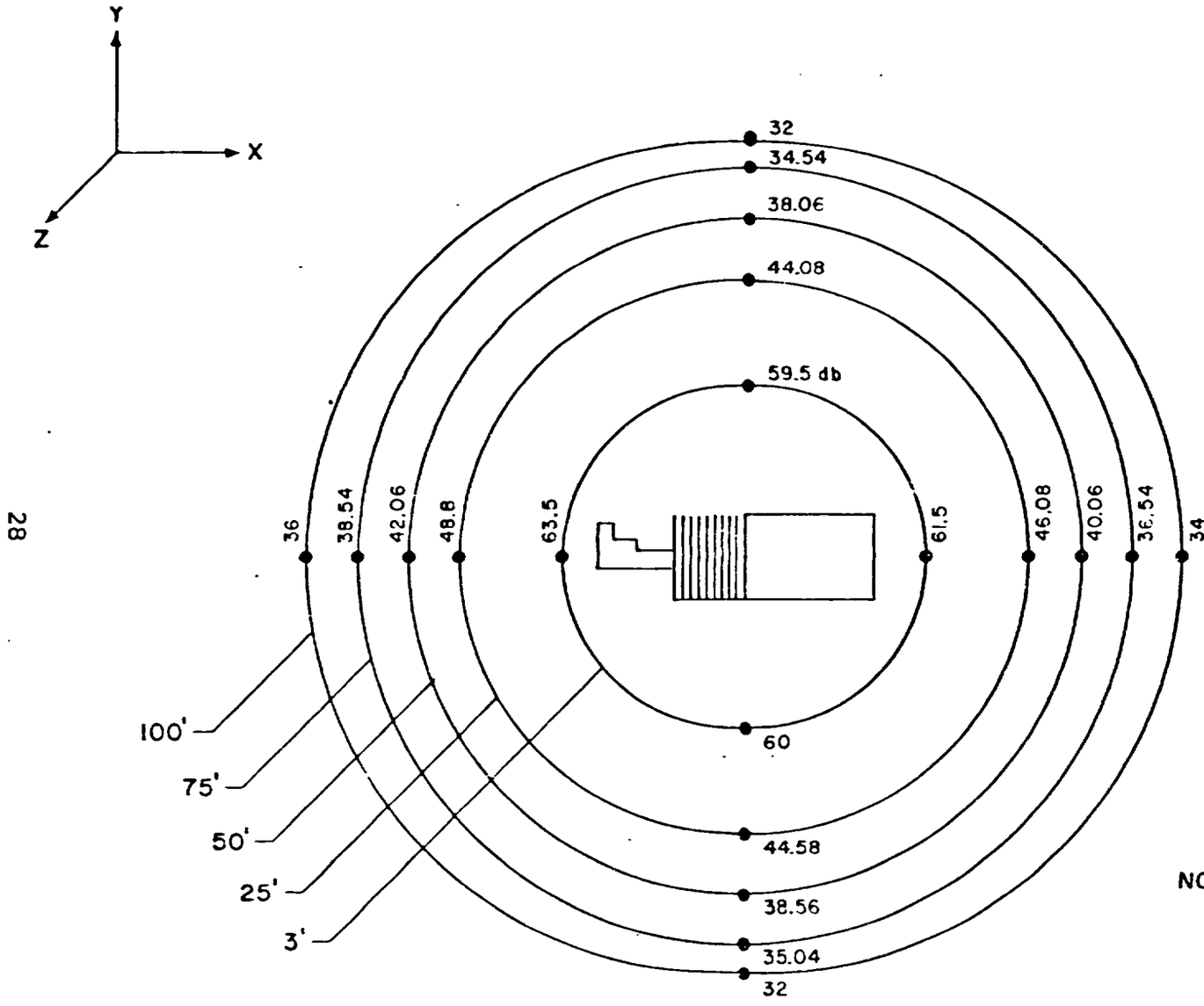

3'	64
25'	48.58
50'	42.56
75'	39.04
100'	35.5

NOTE:
CIRCULAR CURVES REPRESENT
CONSTANT DISTANCES FROM UI
AS INDICATED.
ALL OTHER NUMBERS ARE dbA
REFRIGERATOR RIGIDLY MOUNT
TO 2'X2'X 1/2" LAMINATED PL
NORMAL TO PLATE IS IN Z DIRE

Figure 2: Acoustic Noise Levels at Various Refrigerator Orientations

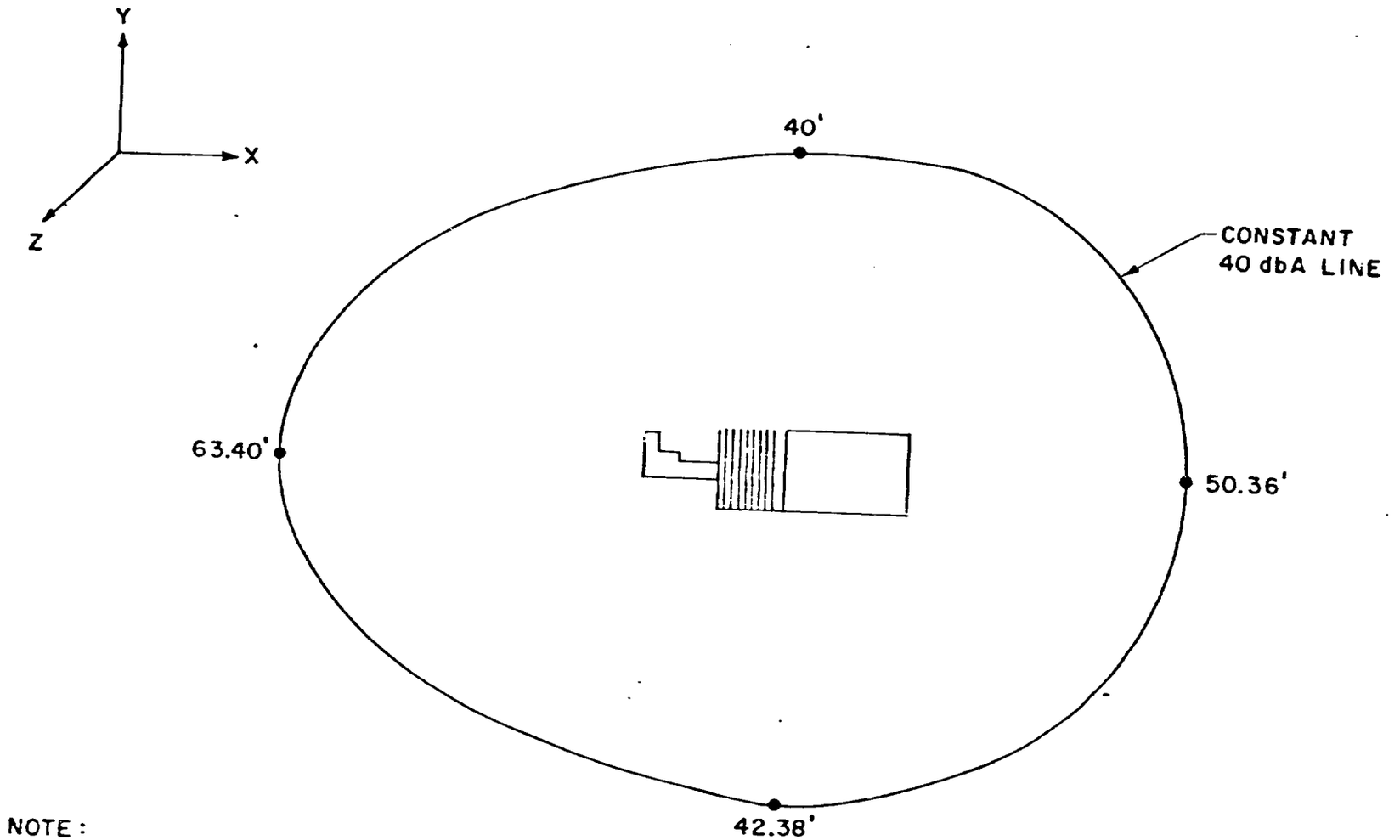

Figure 3: Distances at Which Plate-Mounted Refrigerator Becomes Marginally Audible to the Human Ear

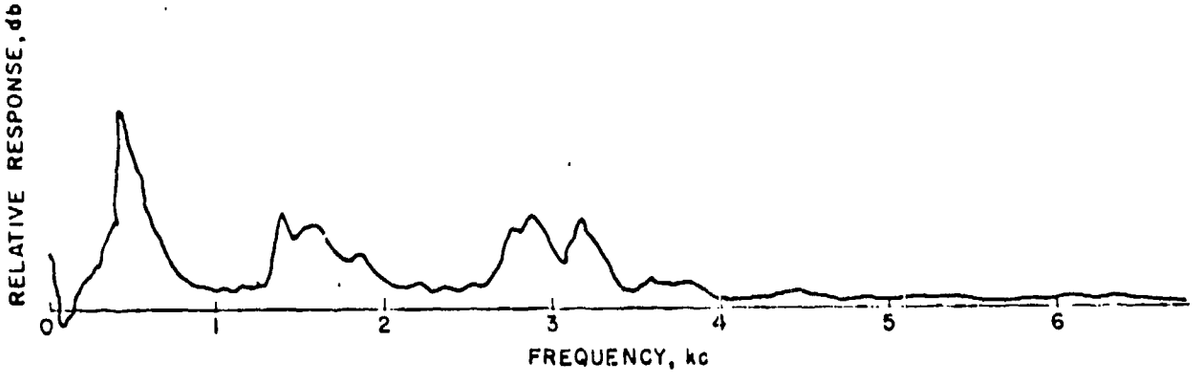

Figure 4: Relative levels of Generated Noise vs. Frequency

2.2.5 Helium Integrity

Based on a limited number of tests, it was determined that the leakage rate is approximately equivalent to 5% loss of charge pressure in 25 days.

2.2.6 Motors

The brushless dc refrigerator drive motors were supplied by Aeroflex Laboratories. They were installed in a test fixture (Fig. 5), and an efficiency test was performed using a Chatillon absorption dynamometer. The results are tabulated in Table 3. As seen from the table, with a power input between 52 to 63 watts (which corresponds to the shaft power range of the refrigerator), the motor efficiency is between 44.2% and 44.68%.

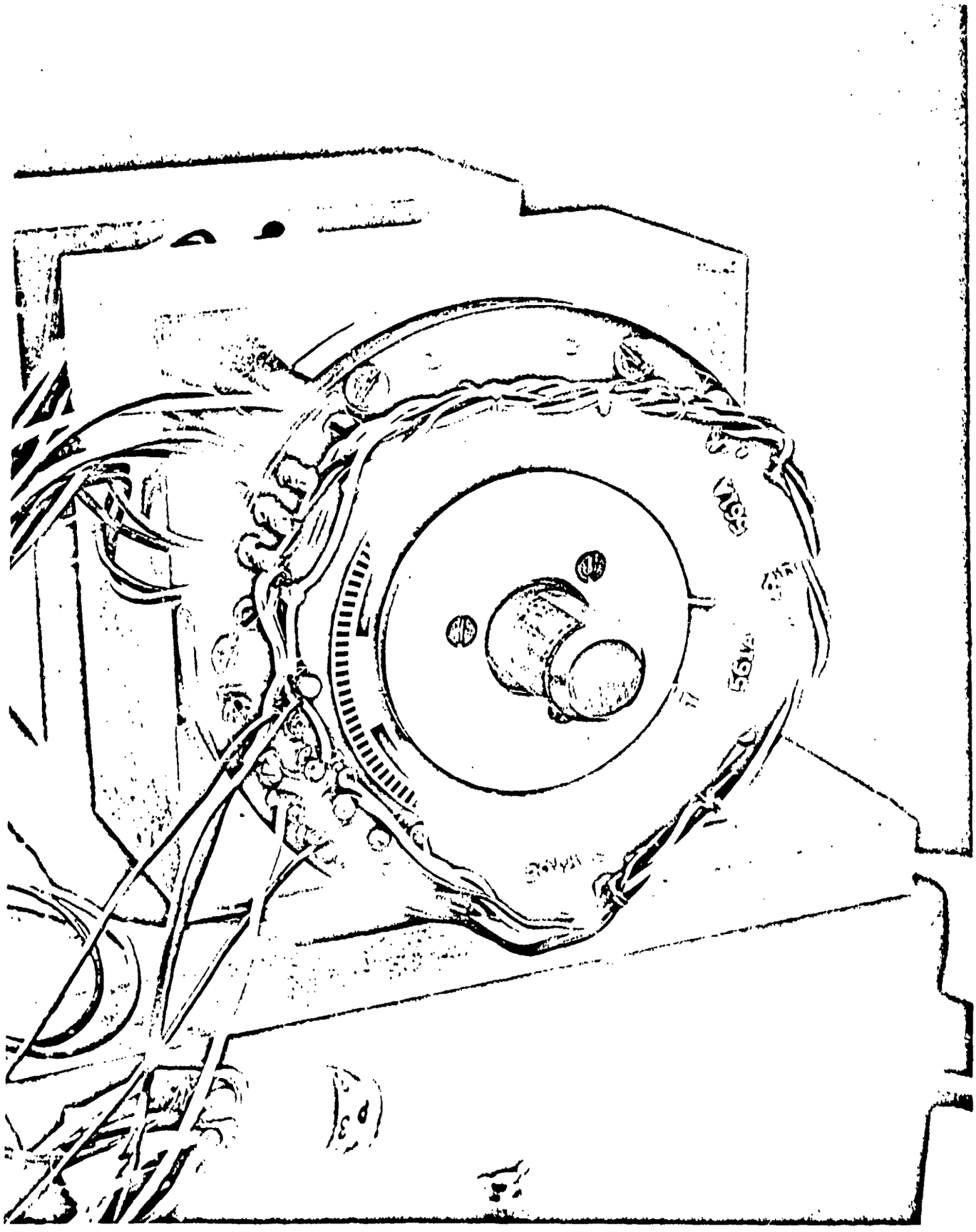

Figure 5: Drive Motors in Test Fixture Showing Motor Position Sensors

Table 3
Performance Data for Brushless and Brush-type Motors

AEROFLEX MOTORS (BRUSHLESS D.C. MOTORS)

TORQUE (INCH-OUNCES)	N(R.P.M.)	VOLTS	AMPS.	P(IN) WATTS	P(OUT) WATTS	EFF. %
6.1	1500	24.1	0.85	20.49	6.77	33.04
11.1	1480	24.0	1.35	32.4	12.16	37.53
16.1	1480	23.9	1.83	43.74	17.63	40.31
21.1	1475	23.7	2.21	52.2	23.07	44.2
26.1	1462	23.65	2.68	63.49	28.37	44.68
31.1	1450	23.55	3.1	73.01	33.37	45.71

MAG TECH MOTORS (BRUSH D.C. MOTORS)

6.1	2070	24	0.73	17.52	9.34	53.3
11.1	1930	↓	0.98	23.52	15.85	67.4
16.1	1810		1.31	31.44	21.55	68.6
21.1	1580		1.67	40.08	26.22	65.4
26.1	1560		2.02	48.48	30.12	62.1
31.1	1430		2.36	56.64	32.9	58.1

2.3 Description of Refrigerator

A photograph and two drawings of the refrigerator are shown in Figures 6, 7, 8. Other subassemblies and parts such as the regenerator, counterweights, piston, displacer rod, rhombic mechanism, and rhombic support housing are shown in Figure 9. This housing enables the rhombic drive to be assembled outside of the crankcase. The final weight of the refrigerator including two electrical plugs is 8 lbs. 7 ounces; its dimensions are 5 7/8" x 5 5/16" x 9 1/4". The electronic controller for the brushless motors weighs 3 lbs. 5 ounces.

A number of different materials were used to fabricate the refrigerator. Magnesium was used to construct the crankcase because of its low density. A low density metal with a relatively high thermal conductivity was needed to fabricate the heat exchanger, hence aluminum was chosen. The heat exchanger was then hard anodized. The regenerator was constructed of titanium because of its low thermal conductivity and strength. The side walls of the cold finger (Fig. 10) were also made out of titanium so that any expansion or contraction between the regenerator and cold finger due to changes in temperature would be negligible. Copper was used on the cold spot (freezer cap) because of its high thermal conductivity. The connecting links were made from stainless steel, the displacer rod was made from oil-hardened tool steel, and the flexible rod from high-strength steel. Three Feuralon AW bushings were incorporated into the unit: two inside the piston where the displacer rod reciprocates, and the other on the bottom crankcase cover to guide and align the displacer rod. Beneath

the regenerator is a cylinder (Figure 9) which contains a flexible support rod. One end of this cylinder is screwed into the displacer rod, while the other accepts the regenerator. The flexible rod in the cylinder allows for any misalignment that may exist. Also located on the cylinder are three Feuralon-AW pads which aid in alignment and prevent the cylinder from making metal-to-metal contact with the heat exchanger wall.

Two sensors are included with the refrigerator, viz., an elapsed time meter powered by the 24 Vdc power source, and a pressure transducer rated for 200 psig with a maximum pressure of 400 psig. To determine operating speed and the position of the displacer, two signals are provided from the electronic controller. The speed signal is a voltage proportional to the operating speed. The displacer position signal is obtained when a glass encoder disk intermittingly interrupts a light beam (produced by a light emitting diode), thereby activating a switching circuit (Fig. 5). This disk contains 127 equally spaced windows along its outer circumference. When a window appears in front of one of the light sensors, the light shines through the window and is sensed by a detector. Consequently, when a window does not appear (blank spacing between window) no light rays are picked up by the detector and hence a voltage spike occurs. Since there are 127 equally spaced windows, 127 voltage spikes will occur. One of the windows in the glass disk, has been covered over, resulting in a reference spike once per revolution. This larger spike can be used as a reference point, so that a relationship between the angular position of the crankshaft and the linear position of the displacer yoke can be obtained.

The following equations show how this angular position information can be converted into the linear position of the displacer. Figure 11 shows a plot of this equation.

$$X_d = r \sin \psi + L \cos \chi$$

$$\frac{X_d}{r} = \sin \psi + \frac{1}{\lambda} \cos \chi$$

and

$$\frac{1}{\lambda} \cos \chi = \sqrt{\frac{1}{\lambda^2} - (\epsilon - \cos \psi)^2}$$

where

$$\epsilon = \frac{e}{r} = 2.53$$

$$\frac{1}{\lambda} = \frac{L}{r}$$

crank radius $r = 0.118$ in.
link length $L = 0.513$ in.
eccentricity $e = 0.298$ in.

and

$$\frac{X_d}{r} = \sin \psi + \sqrt{\frac{1}{\lambda^2} - (\epsilon - \cos \psi)^2}$$

$$X_d = r \left[\sin \psi + \sqrt{\frac{1}{\lambda^2} - (\epsilon - \cos \psi)^2} \right]$$

$$X_d = 0.118 \text{ in.} \left[\sin \psi + \sqrt{18.9 - (2.53 - \psi)^2} \right]$$

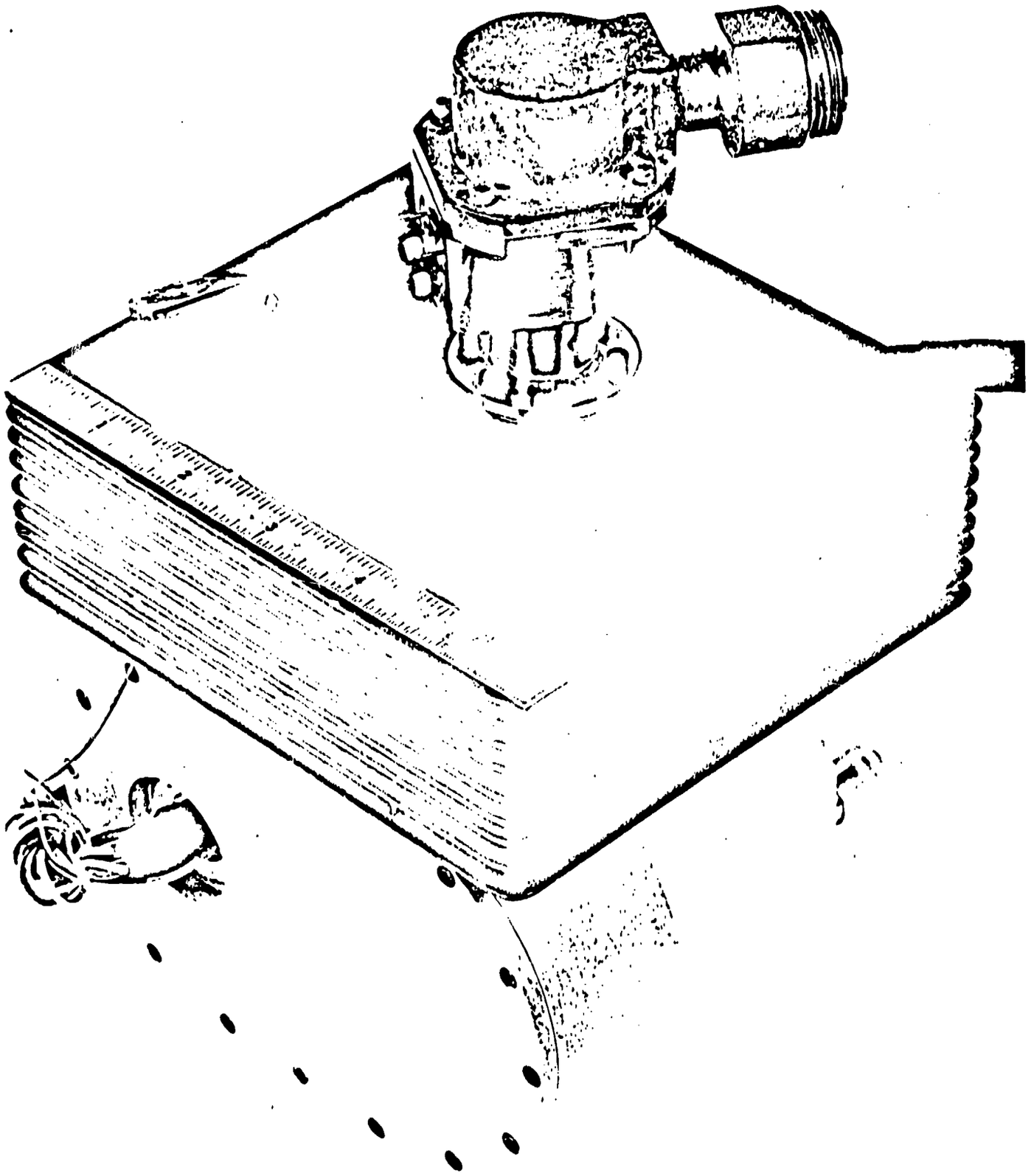

Figure 6: Rhombic Drive Stirling Cycle Refrigerator with Demountable Test Dewar

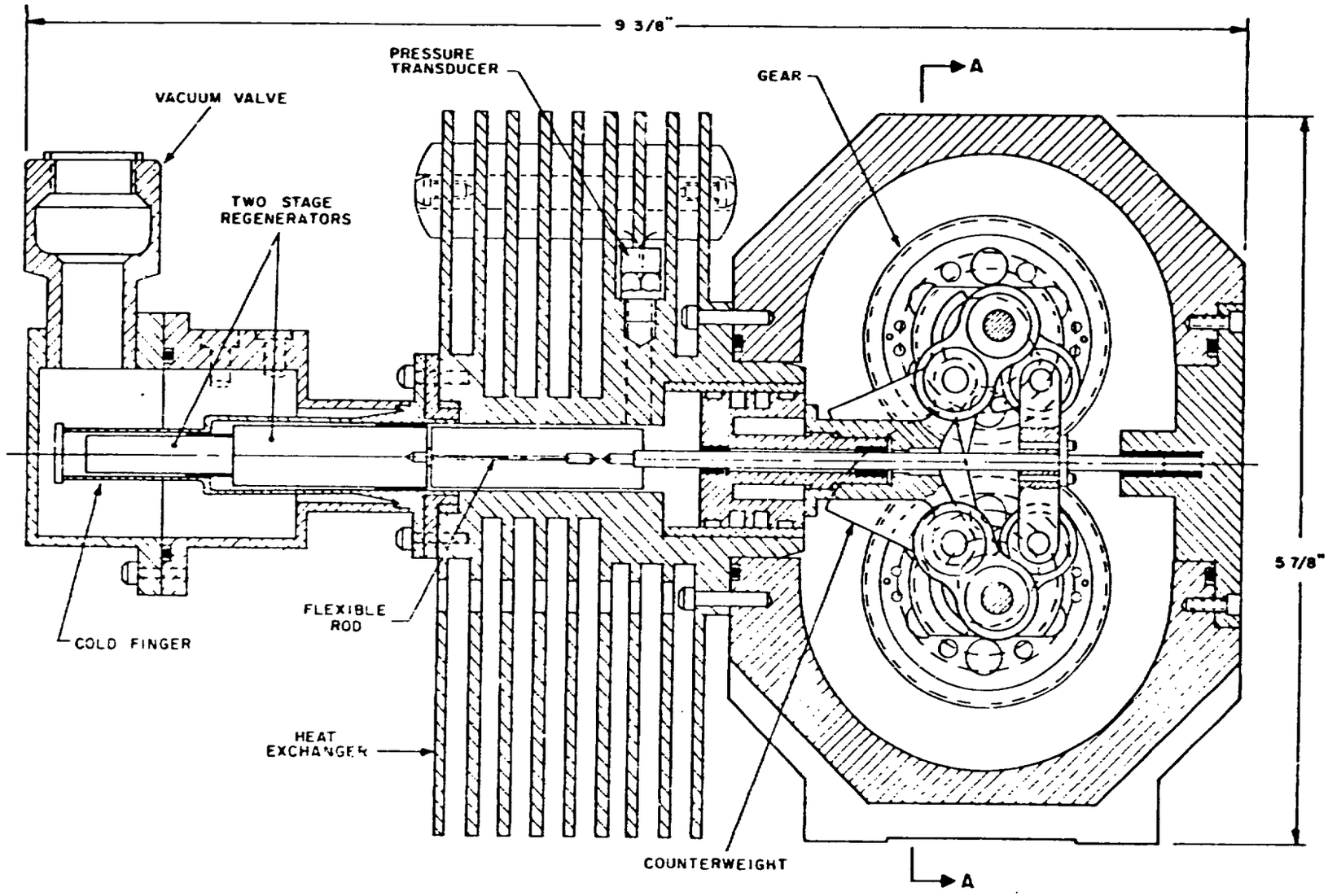

Figure 7: Assembly Drawing of Refrigerator

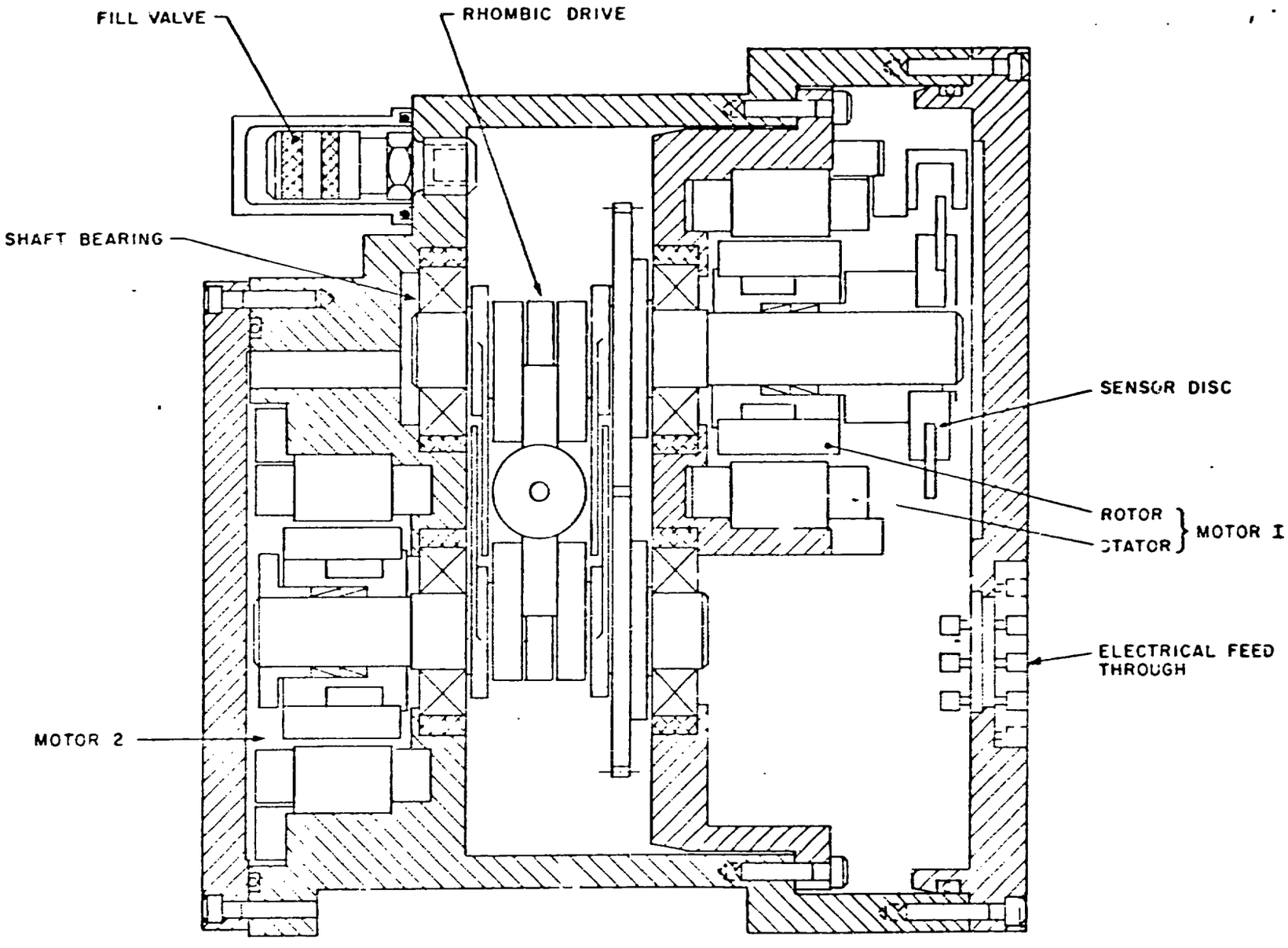

Figure 8: Section View of Refrigerator Crankcase

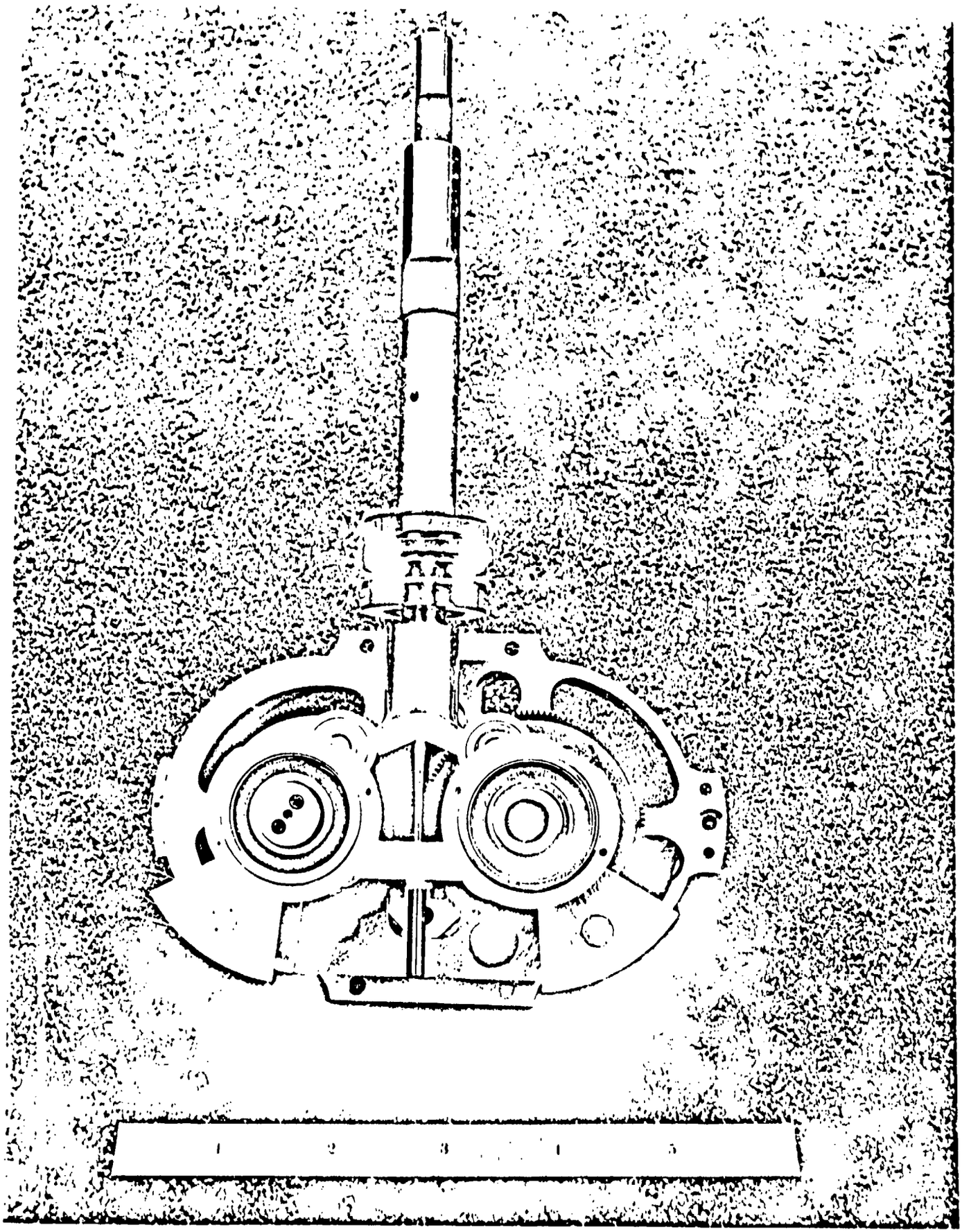

Figure 9: Rhombic Drive in Support Housing and Piston and Displacer/Regnerator

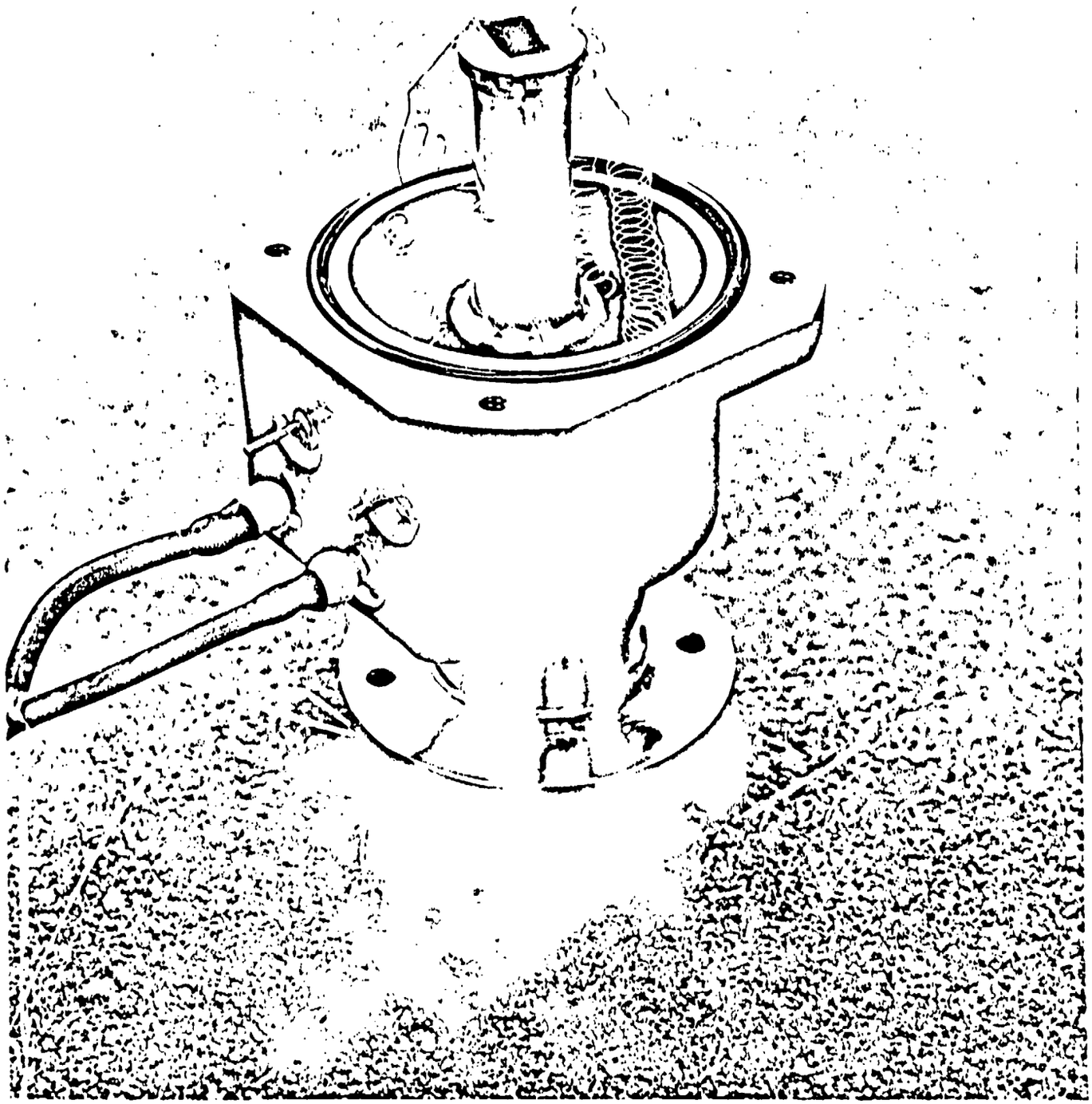

Figure 10: Test Dewar with Cover Removed Showing Cold Finger with Heating Element and Thermocouple

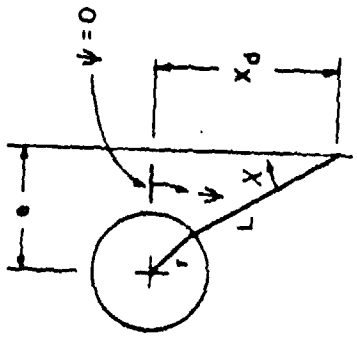

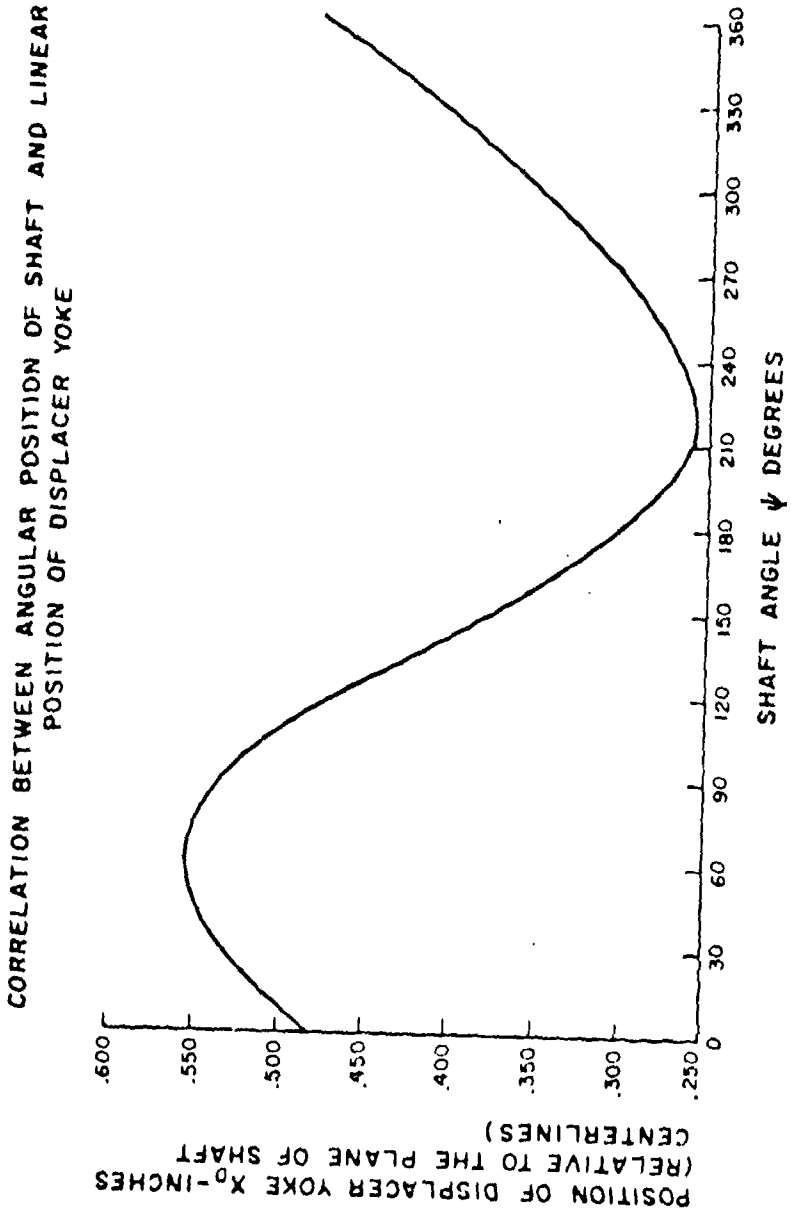

Figure 11: Correlation Between Angular Position of Drive Shaft and Linear Position of Displacer

3. DISCUSSION

3.1 General

As stated in Paragraph 2.2, the maximum pressure ratio was obtained with a Bal piston-to-cylinder seal. This seal also gave the minimum amount of friction losses. To insure meeting the 3,000 hr life, a glass fill was added to the teflon seal material and, to keep the friction at a minimum, molybdenum disulfide was also added. The Feuralon AW seal between the piston and the displacer rod showed no sign of wear, and the Feuralon AW-lubricated bearings appeared under microscopic examination to have proper transfer films on the balls and races with no sign of wear.

The use of a low conductivity titanium alloy (2.5 Sn, 5Al) in both the cold finger and displacer regenerator along with the Kel-F plug in the first regenerator stage was effective in reducing conduction losses while maintaining strength and seal integrity. The flexible rod supporting the regenerator, while allowing it to center itself, was effective in reducing friction between the regenerator seal and the cold finger walls.

As shown in the tables in Paragraph 2.2, the refrigerator is capable of producing 1 watt of cold at 77°K ± 5°K in the 125°F still-air ambient. The shaft power required is only 25 watts and the heat exchanger performs adequately in any orientation. It is also evident that cold production and shaft power required are functions of charge pressure; and that a cold production of 1 watt at the extreme of 77°K + 5°K could be obtained with a charge pressure lower than that reported in Paragraph 2.2. As a result the shaft power would also be lower.

The overall high power consumption of the refrigerator and the marginal ability to perform at the -65°F ambient are the result of the brushless drive motor being inefficient and unable to reliably produce the torque needed to overcome the friction at the low ambient. The vendor has supplied motors with an efficiency of 44.2% to 44.68% (see Table 3, Par. 2.2.6) as opposed to the 55% to 60% contractually required. Also shown in this table are performance characteristics for brush-type motors that will fit into the cavities occupied by the brushless motors and which weigh less. These motors are available as an alternative to the brushless motors. They will solve the problems of high power consumption and unreliable operation at low ambients, but at the cost of added contamination and uncertain life resulting from brush wear.

The acoustic noise data as presented in Paragraph 2.2 shows that the refrigerator, even when fixed to a rigid plate, more than meets the required specifications for inaudibility at 100 ft. against a 40 dbA background. It should be noted that in addition to all the conservative assumptions (described in Par. 2.1.1) made in arriving at these values for noise level, the noise measurements at 3 ft. distance were taken in a closed room approximately 25' x 25' x 10'. This is yet another conservative measure which implies that the data reported represents extreme maximum values for noise levels and for distances at which the refrigerator becomes marginally audible.

The low values for cooldown time reflect the small amount of mass on the cold finger. Cooldown obviously will vary with different amounts of mass added to the finger.

The weight of the machine is within specifications and the size is considerably below specification. Both these properties can be further reduced in the next generation of this refrigerator.

Vibration of the cold finger was not measured directly due to a lack of available time. The levels, however, were judged to be at or below those of previously acceptable refrigerators.

The actual life of the machine remains to be determined.

3.2 Failure Rate

During the initial break-in and testing period, there were failures associated with the refrigerator. Their cause and correction are as follows:

Kel-F bushings on main bearings. In the initial break-in period, it was found that two of the four Kel-F bushings that surround the main bearings had worked loose and contacted the counterweights. The solution was to simply secure these bushings in place by a thin metal bracket. This bracket is held in place by two screws mounted to the case housing of the inner motor. This method proved successful and no further problems were encountered with the bushings.

Regenerator seals. As seen in Figure 9, there are Rulon seals epoxied to the lower portion of each stage of the two stage regenerator. During the initial break-in period, it was noticed that either one and sometimes both of these seals would break off. This would drastically hamper cold production and would also cause an increase in power consumption. It was felt that the reason why the seals were not remaining in place was

The weight of the machine is within specifications and the size is considerably below specification. Both these properties can be further reduced in the next generation of this refrigerator.

Vibration of the cold finger was not measured directly due to a lack of available time. The levels, however, were judged to be at or below those of previously acceptable refrigerators.

The actual life of the machine remains to be determined.

3.2 Failure Rate

During the initial break-in and testing period, there were failures associated with the refrigerator. Their cause and correction are as follows:

Kel-F bushings on main bearings. In the initial break-in period, it was found that two of the four Kel-F bushings that surround the main bearings had worked loose and contacted the counterweights. The solution was to simply secure these bushings in place by a thin metal bracket. This bracket is held in place by two screws mounted to the case housing of the inner motor. This method proved successful and no further problems were encountered with the bushings.

Regenerator seals. As seen in Figure 9, there are Rulon seals epoxied to the lower portion of each stage of the two stage regenerator. During the initial break-in period, it was noticed that either one and sometimes both of these seals would break off. This would drastically hamper cold production and would also cause an increase in power consumption. It was felt that the reason why the seals were not remaining in place was

that either the epoxy used (Bondmaster M777) was beyond its shelf life or that the outer surface of the regenerator was not properly prepared to accept the epoxy and seal. The solution to this problem was to purchase a new supply of epoxy and to properly prepare the outer surface of the titanium regenerator where the seals are fastened. This was done by etching the regenerator surface using a solution of Pasa-Jell 107. The Pasa-Jell is specifically made to improve the metal bond adhesion of titanium alloys. The surface was also sandblasted and scored in a lathe using a thin cutting tool. After preparing the surface by this method and using the new epoxy, the two Rulon seals remained firmly in place throughout the remainder of the testing.

Displacer rod. The displacer rod which is securely fastened to the lower yoke and controls the motion of the regenerator, experienced a slight bending in early operation of the refrigerator. It was felt that the rod was too thin (0.125" dia.) and could easily be bent out of alignment. The solution was to redesign the rod. A thicker rod (0.156" dia.) was made with a flange that was securely fastened into the lower yoke for greater alignment and strength (Figure 9).

Delrin gear teeth. These teeth were not totally constrained to rotate in a single plane. A thin retaining plate was added on one side of the gear hubs to insure that they did.

Brushless drive motors. One light emitting diode, assorted transistors and operational amplifiers, and other components in the logic circuit failed during alignment and operation at

the ambient temperature extreme. It was felt that the majority of these failures were due to high voltage and current spikes; the circuits were repaired and modified where possible and a conservatively valued fuse (4 A) was added.

3.3 Economic Analysis

Based on adjusted machining costs (assuming more economical lot production techniques will be used where applicable) and on estimated motor costs, the following estimate is made for refrigerator lots of 500 and 1,000:

	Cost per Refrigerator	
	500 lots	1000 lots
With brushless motor*	$3000	$2500
With brush-type motor	$2500	$2000

*It is assumed that adequate motors will be used.

4. CONCLUSIONS

The main purpose of this program was to develop an inaudible, Stirling cycle refrigerator. The acoustic noise specification of inaudibility at 100 ft. against a 40 dbA background was bettered. Weight was at specification and size was well below it. Cooldown times were closer to design goals than to specifications. Vibration levels were judged to be acceptable, and refrigerator orientation did not affect vibration, noise or cooling capacity. The refrigerator was capable of cooling and maintaining a one-watt heat load at 77°K ± 5°K when at the 125°F ambient. The brushless drive motors used to power the refrigerator were only 44% efficient (this was below the specification accepted by the motor vendor) and, as a consequence, the refrigerator consumed too much power. The shaft power consumed by the refrigerator, however, was below 26 watts when producing 1 watt of cold at 77°K ± 5°K at the 125°F ambient. This shows that a 62% efficient drive motor would bring the power consumption within specifications. These inefficient brushless motors were also incapable of reliably developing sufficient torque to operate the refrigerator at the -65°F ambient. With the exception of the deficiencies caused by the drive motors, the refrigerator met or exceeded all specifications.

5. RECOMMENDATIONS

- Perform statistically significant life tests on this and/or similar refrigerators.

- Modify the crankcase design slightly to minimize the effect of brush contamination and investigate brush-type dc drive motors.

- Procure sensitive dynamic balancing equipment so a more precise balance of the total machine can be obtained.

- Develop an even smaller, quieter, lighter weight refrigerator with similar efficiency and performance.

- Develop a similar machine with a longer life by utilizing unsupported metal bellows and an oil-lubricated drive.

6. REFERENCES

(1) I. Rudnick, "Propagation of Sound in the Open Air", Handbook of Noise Control, C. M. Harris, Ed., Chapter 3, pp. 3-1 to 3-17, McGraw Hill (1957).

(2) F. M. Wiener, "Sound Propagation Outdoors", Noise Reduction", Chapter 9, pp. 185-205, L.L. Beranek, Ed., McGraw Hill, (1960).

(3) G. K. Pitcher, "Development of Spacecraft Vuilleumier Cryogenic Refrigerators", Interim Report, Part I, December 1971, Air Force Flight Dynamics Laboratory, Air Force Systems Command, Wright-Patterson AFB, Ohio.

(4) Ibid., Part II, July 1972.

(5) F. J. Riha, III, "Development of Long Life, High Capacity Vuilleumier Refrigeration System for Space Applications", July 1971, Air Force Flight Dynamics Laboratory, Air Force Systems Command, Wright-Patterson AFB, Ohio.

(6) Ibid., Part II, November 1971.

APPENDIX A

BASIC THEORY OF THE STIRLING CYCLE REFRIGERATOR

n this section a brief outline of the basic principles of the tirling cycle is presented.[1,2] From an elementary theory the eneral properties of the cycle will be derived with a discussion f the most important losses. It should be noted that the pre-entation is essentially taken from Part Two of reference 1. For more extensive treatment of the subject reference should be made o the original paper[3].

ındamental Cycle

ı the ideal Stirling cycle, the cold is produced by the reversible cpansion of a gas. The gas performs a closed cycle, during which : is alternately compressed at ambient temperature in a compression ɔace and expanded at the desired low temperature in an expansion ɔace, thereby reciprocating between these spaces through one con-ɛcting duct, wherein a regenerator provides for the heat exchange ɛtween the outgoing and the returning gas flow. Figure 1 shows ɛages in carrying out the ideal cycle.

ı this diagram, A is a cylinder, closed by the piston B, and con-ıining a nearly perfect gas. A second piston, the displacer C, .vides the cylinder into two spaces, D at room temperature and E . the low temperature, connected by the annular passage F. This ıssage contains the regenerator G, a porous mass with a high heat ıpacity; the temperature in the passage is shown in the graph. ıe cycle, consisting of four phases, runs as follows:

I Compression in space D by the piston B; the heat of compression is discharged through the cooler H.

Dr. J. W. L. Köhler "The Gas Refrigerating Machine and Its Position in Cryogenic Technique," Progress in Cryogenics 2, 41-67 (1960) London, Heywood and Company Ltd.

A. Daniels, "Cryogenics for Electro-Optical Systems," Electro-Optical Systems Design, vol. 3, pp. 12-20, July 1971.

J. W. L. Köhler and C. O. Jonkers, Philips Tech Rev. 16 69-78, 105-115 (1954)

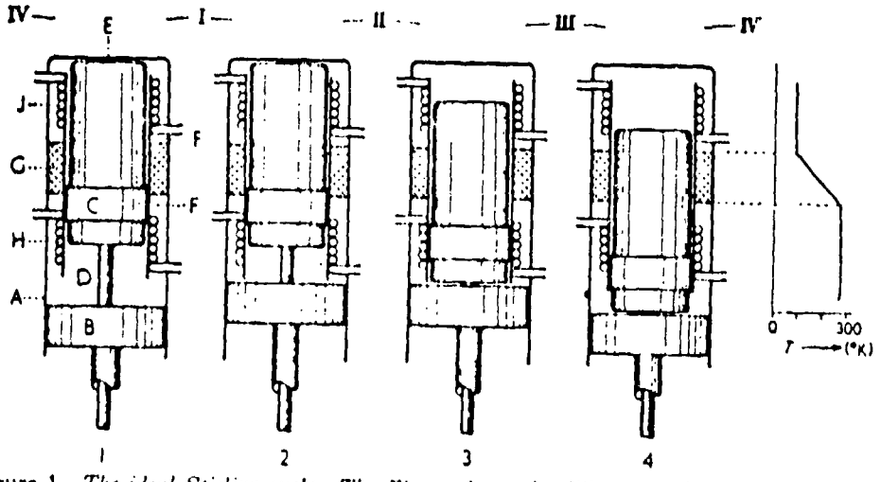

Figure 1. *The ideal Stirling cycle. The Figure shows the different positions 1–4, according to Figure 2. I–IV refer to the four phases of the cycle. The graph on the right shows the temperature distribution in the machine*

II Transfer of the gas through the regenerator to space E by movement of the displacer. The gas is reversibly cooled down in the regenerator, the heat of the gas being stored in the regenerator mass.

III Expansion in the cold space by the combined movement of the piston and the displacer; the cold produced is discharged through the freezer J, and utilized.

IV Return of the gas to space D; thereby the gas is reheated, the heat stored in the regenerator being restored to the gas.

With no regenerator present the gas flowing to the expansion space would arrive there at ambient temperature, whereas the returning gas would arrive in the compression space at the low temperature; this effect would cause such a tremendous cold loss that the whole process would become futile. In an ideal regenerator, a temperature gradient is established in the direction of the gas flow. This causes the gas to be cooled down reversibly, so that it arrives in the expansion space with the temperature prevailing there.

Figure 2 shows the p-V diagram of this schematic cycle, neglecting the dead space. It consists of two isotherms and two isochores; at T_C (compression temperature) the amount of heat Q_C is rejected, at T_E (expansion temperature) the amount of heat Q_E is absorbed.

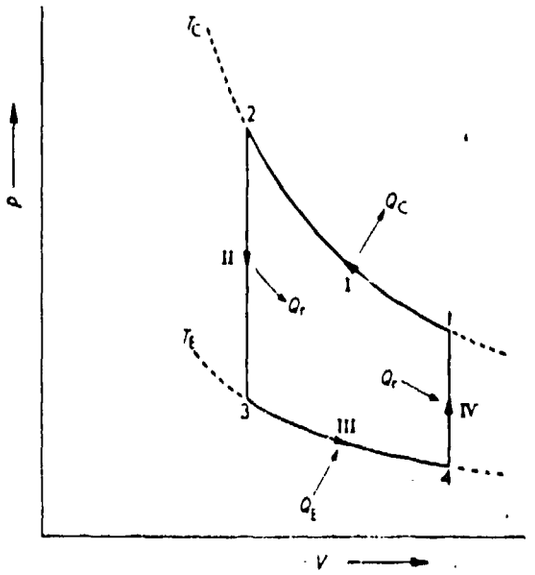

Figure 2. p-V *diagram of the ideal cycle between the temperatures* T_C *and* T_E, *where the amounts of heat* Q_C *and* Q_E *are discharged and absorbed, respectively. The heat* Q_r, *rejected in phase II, is stored in the regenerator and absorbed in phase IV*

Actually, the discontinuous movement of the pistons is difficult to achieve. In practice, the pistons are actuated by a crank mechanism and are thus moving harmonically; for the machine to act as a refrigerator, the expansion space E (Figure 1) has to lead in phase with respect to the compression space D. The harmonic motion and the volume of the heat exchangers (the so-called 'dead space') cause the four phases of the cycle to merge somewhat, so that they cannot be distinguished very well; the gas is not exclusively compressed in the compression space, but also in the expansion space, and the same holds for the expansion. It can be shown however that the difference in output between the discontinuous and the harmonic process is only a few percent.

The fundamental cycle is explained here with the help of the displacer machine. The reason is that actual machines are also of this type. It will be obvious, however, that the cycle may be described more generally by two synchronously changing volumes interconnected by a cooler, a regenerator, and a freezer, whereby the volume that is leading in phase becomes the expansion space wherein the cold is produced. Formulae for the pressure variation, the refrigerating capacity, and the shaft power for this general case will be given in the next section.

Performance of the Ideal (Isothermal) Cycle

In the ideal machine, the thermal contact in the heat exchangers is assumed to be perfect, so that the gas temperature there is equal to the temperature of the walls; the same temperature is supposed to prevail in the adjoining cylinders, which temperatures thus are constant with time. The regenerator is also assumed to be perfect, so that no regeneration loss occurs and the gas temperature there is also constant with time. The working fluid is supposed to be a nearly perfect gas; this condition can be met sufficiently by using hydrogen or helium in practice.

(1) Pressure variation. For the expansion space V_E (temperature T_E) and the compression space V_C (temperature T_C) we write

$$\left.\begin{aligned} V_E &= \tfrac{1}{2} V_0 (1 + \cos\alpha) \\ V_C &= \tfrac{1}{2} w V_0 [1 + \cos(\alpha - \phi)] \end{aligned}\right\} \qquad (1)$$

where V_0 is the maximum volume of the expansion space, w the ratio of the swept volumes of the compression and the expansion space, and ϕ the phase difference between these spaces; the crank angle α (= 0 for $V_E = V_{max}$) changes linearly with time ($\alpha = \omega t$). The volumes of the freezer, the regenerator, and the cooler, which form the connecting channel (the dead space), will be indicated by V_S with the corresponding temperature T_S. The variation of the pressure p with time (or α) now follows from the condition that the mass of the system as a whole is constant:

$$\frac{M}{R}p\left[\frac{V_E}{T_E}+\frac{V_C}{T_C}+\sum\frac{V_s}{T_s}\right] = \text{constant} = C.\frac{M}{R}\frac{V_0}{2T_C}$$

ere M is the molecular weight of the gas, R is the gas constant, d C is a constant. After introduction of V_E and V_C from equation) and of the symbols

$$\tau = \frac{T_C}{T_E}, \quad \text{the temperature ratio}$$

and

$$s = \sum\frac{V_s}{V_0}.\frac{T_C}{T_s}, \quad \text{the total dead space}$$

educed to the swept volume of the expansion space V_0 and normal-ed to the temperature of the compression space T_C), this reduces

$$\frac{C}{p} = \tau\cos\alpha+w\cos(\alpha-\phi)+\tau+w+2s$$

his expression is easily transformed into

$$\frac{C}{p} = A\cos(\alpha-\theta)+B = B[1+\delta\cos(\alpha-\theta)]$$

ith the abbreviations

$$A = \sqrt{(\tau^2+w^2+2\tau w\cos\phi)}; \qquad B = \tau+w+2s$$

$$\frac{A}{B} = \delta; \qquad \tan\theta = \frac{w\sin\phi}{\tau+w\cos\phi}$$

he constant A may be interpreted as two times the total change of olume, while B equals two times the mean total volume, both reduced to $_0$ and normalized to T_C. For the pressure p we thus find

$$p = \frac{C}{B}\frac{1}{1+\delta\cos(\alpha-\theta)}$$

which may be written more conveniently

$$p = \frac{p_{max}(1-\delta)}{1+\delta\cos(\alpha-\theta)} = \frac{p_{min}(1+\delta)}{1+\delta\cos(\alpha-\theta)} \qquad (2)$$

with the introduction of p_{max} and p_{min} for the maximum and minimum values of the pressure during the cycle.

Expression (2) shows that the pressure variation with time is not purely harmonic. In practice, the deviation of harmonic behaviour is rather small however (the function is symmetrical with respect to p_{max} and p_{min}, which points are 180° apart), as the value of δ seldom exceeds 0,4. This means that the pressure ratio of this type of machine

$$\frac{p_{max}}{p_{min}} = \frac{1+\delta}{1-\delta}$$

is about 2, a remarkably low value compared with what is normal in refrigerating apparatus. The presence of the phase angle θ shows that the pressure variation is not in phase with the variation of the expansion or the compression space; it is easily checked that its phase is intermediate between that of these spaces ($\theta \rightarrow \phi$ for $\tau \rightarrow 0$). It will be found, for this reason, heat is absorbed in the expansion space and liberated in the compression space. For later reference, given here is the expression for the mean pressure p_m, deduced by integrating the pressure with respect to the crank angle α:

$$p_m = p_{max}\sqrt{\left(\frac{1-\delta}{1+\delta}\right)} \qquad (3)$$

(2) Heat absorption in cylinders. The heat absorbed per cycle in the expansion space (Q_E) and in the compression space (Q_C, a negative quantity) is given by

$$Q_E = \oint p\,dV_E, \quad Q_C = \oint p\,dV_C$$

That these expressions, which are normally used for spaces with a constant gas content, may also be used in the case where gas enters and leaves the space can be proved by an involved thermodynamic reasoning which is omitted here. It is easily seen that the value of the integrals depends only on the components of p which have the same phase as dV_E and dV_C; this means that $0 < \theta < \phi$ if the machine has to operate as a refrigerator. Evaluation of the integrals leads to

$$\left.\begin{aligned} Q_E &= \frac{\pi}{a} V_0 p_m \frac{w \sin\phi}{B} \\ Q_C &= -\tau Q_E \end{aligned}\right\} \qquad \ldots(4)$$

with $\quad a = 1 + \sqrt{(1-\delta^2)} \simeq 2$

For practical use, equation (4) may be transformed into q_E, the heat absorbed per second (or the refrigerating capacity) by inserting n, the number of revolutions per minute. If V_0 is expressed in cm^3, p_m in kg cm^{-2}, and q_E in watts, it is found that

$$q_E = \frac{5 \cdot 136}{a} V_0 p_m \frac{n}{1000} \frac{w \sin\phi}{B} \quad \text{(in watts)} \qquad \ldots(4a)$$

Expression (4a) shows that, besides with V_0 and n, the output is proportional to p_m and inversely proportional to the function B, which was defined as the mean reduced and normalized volume. The consequences of the dependence on the mean pressure and the temperature ratio (τ is also contained in s), which constitutes one of the features of the process, will be discussed at more length later. According to expression (4a) an increase of the dead space s reduces the output, as could be expected. A discussion on the influence of the design constants w and ϕ would be very elaborate and lengthy and is therefore outside the scope of this report; their choise depends largely on the losses of the process.

Shaft power and efficiency. For the work W needed to drive
machine one may write

$$W = -Q_E - Q_C$$

Thus

$$W = (\tau - 1)Q_E = \frac{\pi}{a}(\tau - 1)V_0 p_m \frac{\omega \sin \phi}{B} \qquad \ldots(5)$$

ng equation (5) the efficiency of the cycle is

$$\eta = \frac{Q_E}{W} = \frac{1}{\tau - 1} = \frac{T_E}{T_C - T_E} \qquad \ldots(6)$$

efficiency of the ideal cycle thus equals that of the Carnot
le; this is obvious as the cycle is completely reversible.

hough in actual machines the performance is reduced by losses,
be discussed in the next section, the ideal cycle has to be con-
lered as the reference process, because most essential facts
be deduced from it.

ore closing this section two remarks on the representation of
process will be made. The first remark concerns the represen-
ion in a thermodynamic diagram (e.g., p vs V, T vs S, etc.).
se diagrams always relate to a fixed quantity of the working
id, which has to be in internal equilibrium (equal p and T
oughout); this quantity is passed through a number of thermo-
amic states and (at least in a closed system) is returned
timately to its initial state, so that a cycle is described.
king at the Stirling process, it is found that, in so far as
lic behaviour is concerned, nothing abnormal is at hand. How-
r, the system is not homogeneous at all, as different parts of
have a different temperature. As a consequence, different gas
ticles describe completely different cycles between different
peratures; to mention only two extreme examples, some particles
reciprocating between the compression space and a point in the
ler, while other particles are reciprocating between a point in
freezer and the expansion space. That, because of this situa-
n, normal diagrams have lost their value is shown by the fact
t one would have to draw an infinite number of diagrams for the
se particles with different cycles, which obviously leads

owhere. The only diagram which still has some sense is the p-V iagram, as the system is homogeneous in p. But in such a diagram ne is not allowed to draw isotherms or adiabates, as these lines ave lost their meaning. To avoid this difficulty when drawing igure 2, the dead space was assumed to be zero; in that case sotherms may be drawn, since only then the gas is at thermal quilibrium during the compression and the expansion. When the diabatic losses are discussed in the next section, this subject ill have to be returned to. The second remark concerns the escription of the cycle in a schematic form. The transfer of the as from the compression space to the expansion space and vice ersa is performed with constant volume of the gas; this is the implest representation, as the transfer can be effected by ie movement of the displacer only. But this way of transfer is ily one example of a multitude of possibilities which exhibit ie common property that regeneration is possible. As another cample consider transfer at constant pressure, which way of trans- er approximates the harmonic cycle much better. The only reason ny this manner of transfer is not used to explain the cycle is iat it can only be accomplished by simultaneous movement of the ston and the displacer, which obviously is more complicated. iis point is stressed because at many places in literature the ransfer with constant volume is considered to be one of the main iaracteristics of the Stirling cycle, to contrast it with the rcle of Claude (with separate compressor and expander), where ie transfer is performed at constant pressure. explained, this ew does not correctly locate the distinction between the two rcles, the real difference being that in the Stirling cycle the is is reciprocating through one connecting duct, wherein the heat xchange is brought about by regeneration, whereas in the Claude rcle the connecting circuit consists of a counter-flow heat changer (with two channels). Apart from the restriction contained the first remark the Stirling cycle thus closely resembles the aude cycle thermodynamically.

The Actual Cycle

As stated already, the actual cycle differs from the ideal one by the occurrence of losses. For a fuller discussion on this subject reference is made to the original paper[2], here only the most characteristic effects will be treated.

The losses can affect the process in two different ways, viz., by increasing the shaft power and by decreasing the refrigerating capacity; the smaller the ideal values of these quantities, the more pronounced will be the relative effect. Figure 3 illustrates that increase of the shaft power exerts the greatest influence at high refrigerating temperatures, while decrease of the output creates the most adverse effects at low temperatures. In this way a temperature range arises, the "optimum working range", wherein the actual efficiency differs least from the ideal one (i.e., where the figure of merit is highest). This range may be shifted both to higher and to lower temperatures by suitable design; moreover, its limits greatly depend on present and future technological possibilities.

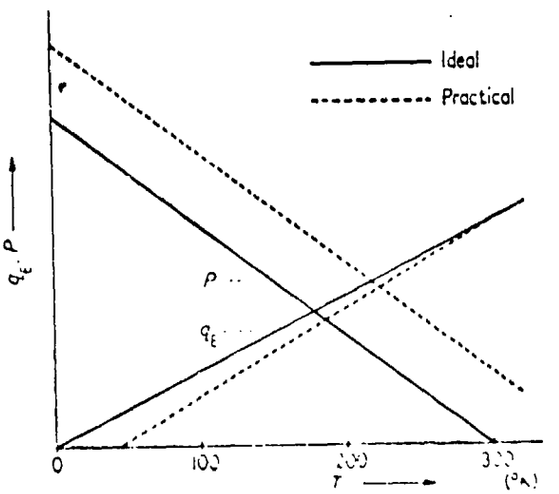

Figure 3. Graphs of the shaft power P and the refrigerating capacity q_E as a function of temperature. The full lines apply to the ideal process, the dotted lines to an actual machine with losses

The increase in shaft power is mainly due to three causes, namely, the mechanical loss of the drive, the flow loss (that is, the power needed to force the gas through the narrow connecting circuit) and the adiabatic loss. The first two losses need no further comment, but the adiabatic loss will be discussed at greater length. In the ideal isothermal process it was assumed that the temperature in the cylinders is constant with time. This means that the thermal contact between the gas and the wall in the cylinder spaces is assumed to be so perfect that these walls can be employed as well to establish the contact between the gas and the surroundings, that is, to serve as cooler and freezer. In this case, separate heat exchangers are of no use and must be omitted; this ideal machine thus consists of the two cylinders and the regenerator and is therefore referred to as the "three-element machine".

Actually, the separate heat exchangers are introduced because the thermal contact between the gas and the cylinder walls is always so poor that insufficient heat exchange with the surroundings can be established through these walls; for this case the name "five-element machine" is used. As a consequence, the temperature of the gas in the cylinders changes nearly adiabatically with time. This adiabatic behavior has only a minor influence on the efficiency (it would be too involved to give the full explanation here; it is based on the fact that these processes occur in both cylinders with the same phase, so that the temperature ratio is independent of time), but in this case the heat (or the cold) must be transported from the cylinders to the heat exchangers. This transport can only be effected by the reciprocating gas which performs it by assuming different temperatures when flowing in opposite directions, with the result that the mean temperature in each cylinder deviates from that in the adjoining heat exchanger. Figure 4 shows schematically the temperature distribution in the machine. It will be observed that the mean temperature in the expansion cylinder is lower than that of the freezer and that the mean temperature in the compression cylinder is higher than that of the cooler. This means that the ratio of the cylinder temperatures is higher than that of the temperatures of the

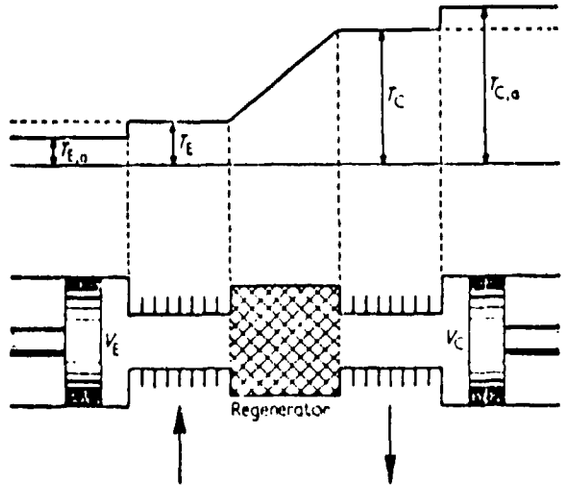

Figure 4. *Temperature distribution in the adiabatic 'five-element machine'. The contact with the surroundings is effectuated by the cooler and the freezer. The mean temperature in the compression space $T_{c,a}$ is higher than the cooler temperature T_c as heat must be transported from the cylinder to the cooler; by the same argument the mean temperature in the expansion space $T_{E,a}$ is lower than that of the freezer T_E.*

heat exchangers, which causes an increase in shaft power. Strictly speaking, the expression "adiabatic loss" is therefore misleading and should be replaced by "transport loss". It is adhered to though, because ultimately the adiabatic behavior is the fundamental cause that has necessitated the introduction of separate heat exchangers. Because the value of the temperature ratio τ is larger in the adiabatic than in the isothermal case, one would expect also a decrease in refrigerating capacity; this influence is very small, however, as the larger value of τ is nearly compensated by a decrease of the quantity B, the mean relative volume of the working circuit, which quantity has another form in the adiabatic case.

In the above discussion the use of the expressions "adiabatic compression" or "expansion has been intentionally avoided. The reason is that the gas is compressed and expanded everywhere in the working space; its behavior during these processes, however, depends largely on the condition of heat transfer prevailing in the various sections of the volume. While in the cylinders the gas temperatures change nearly adiabatically, this is not the case in the connecting circuit;

in the regenerator, for example, the heat transfer is so high, that the behavior is practically isothermal. Thus, while the actual Stirling process is certainly not isothermal, it would be incorrect to call it adiabatic. This situation thus furnishes still another example for the previously made remark that thermodynamic diagrams are of little value for this process.

The decrease of the refrigerating capacity is mainly due to two effects, the flow loss and the insulation loss. Again no comment is made on the flow loss. Also the insulation (and conduction) loss proper needs no discussion. There exists another loss, however, that acts as an insulation loss as well which has the utmost importance for the quality of the process. This loss, caused by the non-ideal behavior of the renerator, will now be discussed.

It is obvious that in the Stirling process ideal regeneration is possible in principle as the same amount of gas passes the regenerator in both directions with the same temperature difference, so that the amount of heat rejected and absorbed by the gas for both directions of flow is the same, since the specific heat is independent of pressure (which is practically the case for nearly perfect gases). The following argument shows the extreme importance of a small departure from ideality of the regenerator, caused by non-ideal heat transfer. In the regenerator a quantity of heat Q_r must be absorbed and rejected in each cycle. Owing to imperfections, this amount is reduced to $\eta_r Q_r$, where η_r is the efficiency of the regenerator. This means that only part of the available heat is transferred to the regenerator. The rest, that is $(1-\eta_r)Q_r$, is carried along with the gas through the regenerator, so that the gas arrives too hot in the expansion space. This remainder, ΔQ_r, thus constitutes the regeneration loss. As this loss must be made up from the cold produced Q_E, it must be compared with this quantity. Calculations show that

$$\frac{\Delta Q_r}{Q_E} = C_r(1-\eta_r)\frac{T_C - T_E}{T_E} \qquad \ldots(7)$$

The constant C_r depends mainly on the compression ratio; its value is approximately 10. For example, take T_C = 300°K, T_E = 75°K, and the regeneration loss $1-\eta_r$ = 1%; then

$$\frac{\Delta Q_r}{Q_E} = 10 \times 1 \times 3 = 30 \text{ per cent}$$

Thus each percent of regeneration loss involves a loss of 30 per cent in refrigerating power; below 30°K this figure even increases to greater than 90 percent, meaning that at such temperatures the entire cold production is consumed by the regenerator. It is thus no exaggeration to call the regenerator the heart of the machine.

The regenerator used in actual gas refrigerating machines consists of a mass of fine metal wire, forming a light felt-like substance. With this type of material, efficiencies of 99 per cent and higher can be obtained; the thermal conductivity of the material is very low.

This section will be ended with a short discussion on the problem of how to minimize the total sum of the losses; this problem is very involved indeed, so that only a very broad outline can be given. As an example, the regenerator will be considered. The losses of the regenerator make themselves felt in three different ways, viz., the regeneration loss (reducing the cooling power), the flow loss, and the dead space (this is not a real loss as the shaft power is also decreased; it exerts its influence through the other losses, as these increase relatively). The regeneration loss can be reduced by making a longer regnerator; this, however, increases the flow loss and the dead space. One may also give the regenerator a larger cross-section; this reduces the flow loss and somewhat the regeneration loss, but increases the dead space. Thus it is possible to find optimum dimensions for the regenerator. The same hold for the freezer and the cooler, where the regeneration loss is replaced by the loss due to insufficient heat transfer. Moreover, the losses are governed by the choice of the values of w and ø. Finally, the

outside of the cooler and the freezer must be made optimal. Thus a very large number of design parameters are to be fixed such that the total result gives an optimum condition; it will be obvious that a lot of experience is needed to find the right solution quickly. This is compensated by the fact that once a system of calculation is worked out, it holds for any size of machine.

APPENDIX B

IMPROVEMENTS TO THE BASIC STIRLING CYCLE: EXPANSION STAGING

EXPANSION STAGING

Equation (7) given in Appendix A for the relative regeneration loss suggests two possible methods for improving the refrigeration process: decreasing the value of C_r and increasing the value of η_r.

The way to decrease C_r would be to increase the compression ratio since C_r depends mainly on this ratio. At present, no practical configurations exist to achieve this so the value of 10 for C_r remains close to a minimum.

The value of η_r, about 99% in typical regenerative refrigerators, can be increased somewhat. Regenerators with efficiencies of 99.5% and higher have been made. However, since a regenerator with such high efficiencies normally has very high flow losses, lower net refrigerator efficiency will result.

To avoid the disadvantages cited above, Philips, in 1963, modified the conventional single expansion system[1]. The modification consisted of thermally staging a number of expansion processes in as many expansion spaces. The method is somewhat analogous to the Keesom cascade process, except that no separate thermodynamic cycles are used, since the complete cycle is performed in one closed system. This modified cycle has been referred to as the "double expansion" cycle.

In this method the expansion is performed in two expansion spaces, each at a different temperature. The spaces are connected in series, with regenerators in the interconnecting passages. The displacer used in the single expansion machine has been adapted to the double expansion process, as shown in Figure 1. The additional, intermediate expansion space M_M is obtained by "stepping" the diameter of the displacer. By virtue of this stepped displacer, volume vari-

---

G. Prast, "A Philips Gas Refrigerating Machine for 20°K," Cryogenics, vol. 3, pp. 156-160, September 1963.

ations of the two expansion spaces (E and M) are in phase. The advantage of this type of construction is that the pressure difference across the seal between the expansion spaces is small, as in the conventional design.

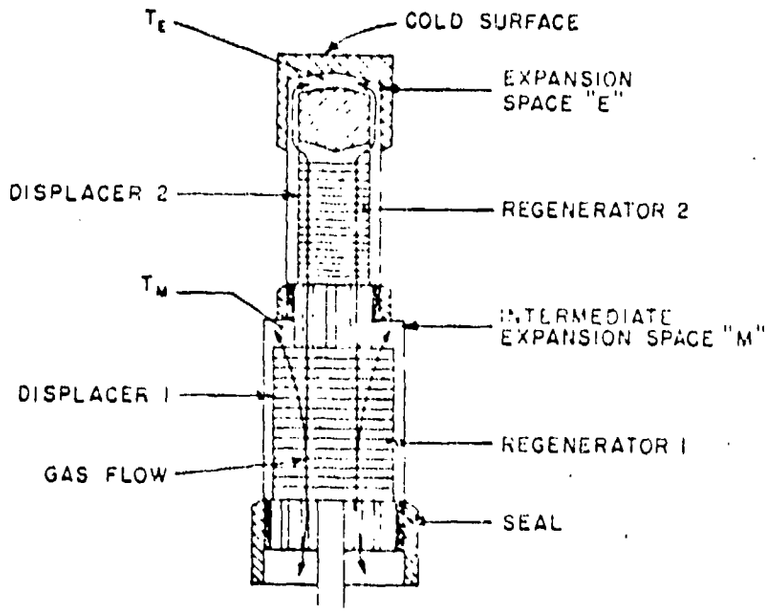

Figure 1: Schematic of typical double expansion configuration

As a result of the additional expansion space, the refrigerator produces cold at two different temperatures, whereas in the conventional process cold production takes place at only one temperature.

The following discussion shows how this system reduces the influence of the regeneration loss. Assume that a mass of working gas m_M is expanded in the intermediate expansion space at a temperature T_M, and that a mass of working gas m_E is expanded in the top expansion

space at a temperature T_E - both gases expanding from a pressure p_1 to a pressure p_2. The ideal cold productions in the expansion spaces are:

$$Q_M = m_M R T_M \ln(p_1/p_2)$$

$$Q_E = m_E R T_E \ln(p_1/p_2)$$

The mass flowing through regenerator 1 between room temperature and the intermediate temperature now is $m_M + m_E$, and the mass flowing through regenerator 2 between the intermediate space and the expansion space is m_E. The regeneration losses for these regenerators are:

$$\Delta Q_{r1} = (m_M + m_E)\, C_p (1 - \eta_{r1})(T_C - T_M)$$

$$\Delta Q_{r2} = m_E C_p (1 - \eta_{r2})(T_M - T_E)$$

Hence the relative regeneration losses are:

$$\frac{\Delta Q_{r1}}{Q_M} = \frac{m_M + m_E}{m_M} C_r (1 - \eta_{r1}) \left(\frac{T_C - T_M}{T_M}\right)$$

$$\frac{\Delta Q_{r2}}{Q_E} = C_r (1 - \eta_{r2}) \left(\frac{T_M - T_E}{T_E}\right) \qquad (1)$$

It should be noted that C_r again has the same value (approximately 10) if p_1/p_2 has the same value.

Now $\Delta Q_{r2}/Q_E$ is small, because T_M is of the order of 140°K, and $T_M - T_E$ is therefore less than $T_C - T_E$, the quantity that occurred in Equation (7) of Appendix A. The consequence is that little of the cold production in the top expansion space is lost, thereby resulting in a relatively large increase in net cold production. When the refirgerator of interest needs cold at one level only, no net

production Q_M is needed, and it is permissible for $\Delta Q_{r1}/Q_M$ to be of the order of unity. Taking the efficiency of regenerator 1 to be 98%, it follows from Equation (1) that:

$$\frac{\Delta Q_{r1}}{Q_M} = 0.2 \frac{m_M + m_E}{m_M}$$

Hence, $(m_M + m_E)/m_M$ can have a value of about 5. This means that in a refrigerator using a double expansion configuration only a mass of about one-fifth of the total mass flowing through the first regenerator needs to be expanded in the intermediate space; this causes only a relatively small increase in the compression work.

It is evident from the foregoing that given the same conditions, i.e., cold production at a given operating temperature, the double expansion configuration is more efficient. There is, however, additional complexity, viz., two regenerators instead of one. It should be noted that an intermediate temperature level in the double expansion configuration offers significant advantages in some cases. For instance, in certain applications where radiation shielding is desirable, the shield can be cooled at the intermediate temperature level. The required refrigeration can of course be produced more efficiently at this level.

The multi-expansion concept has been extended one step further, to a triple-expansion Stirling cycle configuration[2]. In this case, temperatures as low as 7.2°K, with only one cycle, have been attained. A triple-expansion VM refrigerator is presently under development for a spaceborn application[3].

---

[2] A. Daniels and F. K. du Pré, "Triple-Expansion Stirling Cycle Refrigerator," Advances in Cryogenic Engineering, vol. 16, pp. 178-184, June 1970.

[3] G. K. Pitcher, "Development of Spacecraft Vuilleumier Cryogenic Refrigerators," AFFDL TR-71-147, PART I & II, Contract F33615-61-C-1024, December 1971.

APPENDIX C

IMPROVEMENTS TO THE BASIC STIRLING CYCLE: PHILIPS RHOMBIC DRIVE

The Stirling cycle refrigerator has two reciprocating masses: a piston and a low temperature displacer-regenerator. These masses have to be moved in a given phase relationship to each other, i.e., the displacer-regenerator has to lead the piston by approximately 90°. The required motion of these elements is attained with the aid of drive mechanisms.

In addition to imparting the proper phase relationship to the reciprocating masses, the drive mechanism of a Stirling refrigerator should, ideally, lend itself to balancing. This feature is desirable in most applications which incorporate miniature cryogenic refrigerators, since the devices to be cooled cannot, in most instances, tolerate significant vibrational levels without compromising their sensitivity. Another attractive feature of a balanced design is its potentially longer life than that of a mechanism subjected to vibratory loads.

A mechanism which meets the above conditions is the rhombic drive, invented in 1953 at the Philips Research Laboratories in Holland[1].

The rhombic drive converts rotary into reciprocating motion. The rotary input is normally supplied by electric motors, connected to the drive's two identical, parallel crankshafts, which are coupled to each other with gears for synchronous rotation in opposite directions. The crankshafts are located symmetrically about a plane parallel to their axes and passing through the center line of the driven machine.

The mechanism also contains two pairs of connecting rods, each pair driven by a crankshaft with the aid of crank pins; the ends of the connecting rods are interconnected by yokes, which in turn are attached to the elements to be reciprocated.

---

1 R. J. Meijer, "The Philips Stirling Thermal Engine," Ph.D. Thesis, Delft College of Advanced Technology, 1960.

Figure 1 is a schematic diagram of the mechanism. Fixed to piston 1 by way of piston rod 2 is a yoke 3. One end of the yoke is linked by connecting rod 4 to crank 5, the other end by connecting rod 4' to crank 5'. The displacer-regenerator (not shown) is actuated by a similar arrangement: the displacer rod 7, which passes through the hollow piston rod 2, is coupled to a yoke 8 which is linked to cranks 5 and 5' by connecting rods 9 and 9', respectively. If 9 and 9' are given the same length as 4 and 4', the two pairs of connecting rods will form a configuration similar to a rhombus, only the angles of which vary when the system is in motion. Gears 10-10' ensure exact symmetry of the system at all times. Although the two crankshafts are geared together for synchornous movement, power input can be applied either to one shaft using one motor or to both shafts simultaneously using two motors. In the latter case no power is transmitted through the gears.

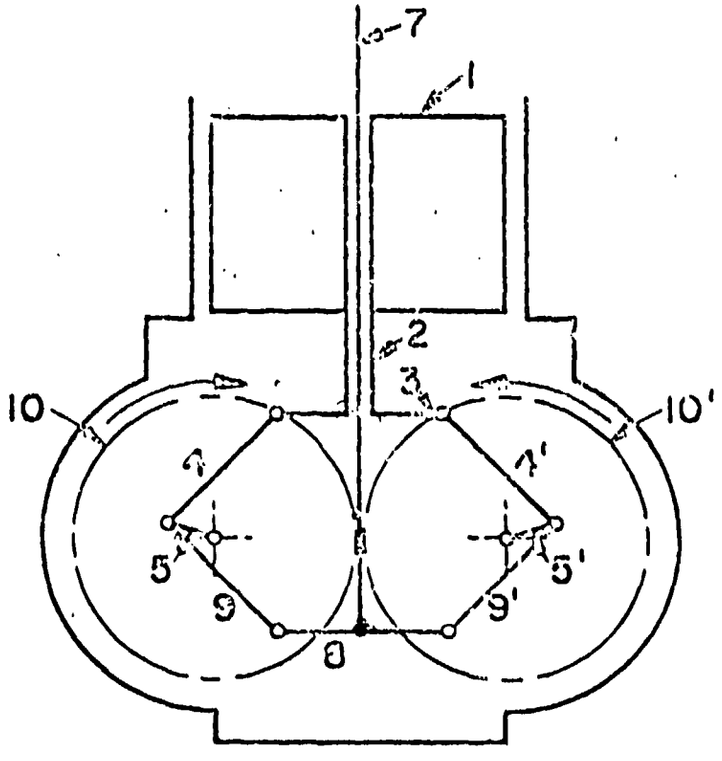

Figure 1: Schematic diagram of conventional rhombic drive mechanism

Figure 2 shows a rhombic drive developed for a miniature Stirling cycle refrigerator[2]. Its motion is illustrated by showing the mechanism in two different positions.

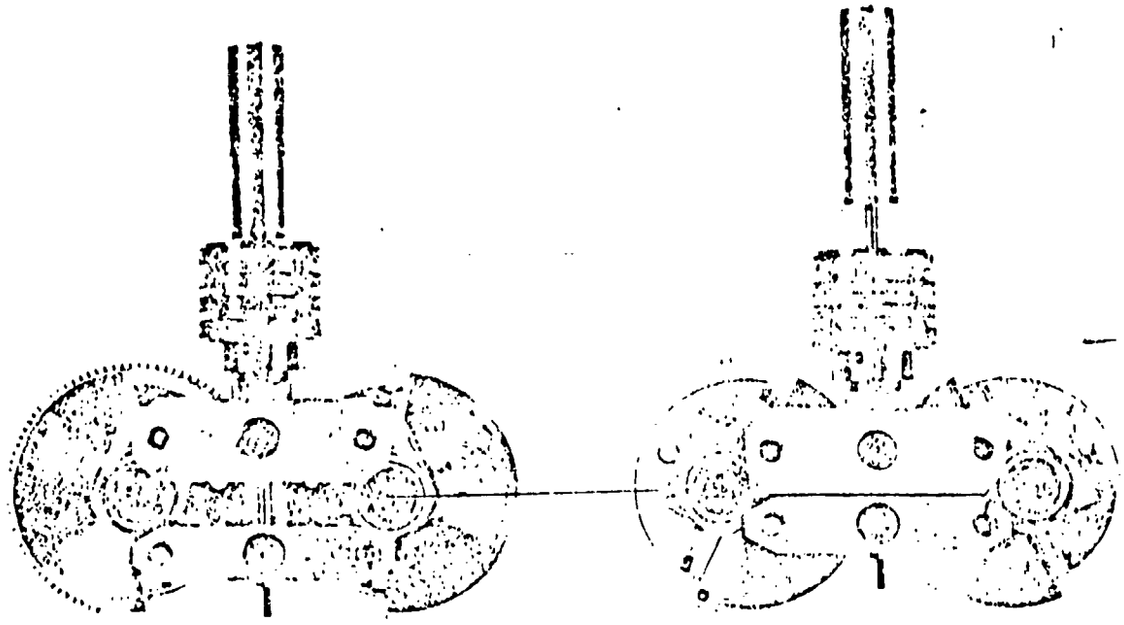

Figure 2: Rhombic drive developed for miniature Stirling refrigerators

The rhombic drive can be completely balanced for all the forces acting on the mechanism and for all their moments - "completely" in the sense that both the fundamentals and all the higher harmonics can be balanced. A rigorous mathematical proof of the drive's dynamic balance is given in Reference 1. A qualitative proof for the simplest case is given below with the aid of the configuration shown in Figure 3.

---

[2] A. Storage, "A Miniature, Vibration-Free, Rhombic Drive, Stirling-Cycle Cooler," Advances in Cryogenic Engineering, vol. 16, pp. 185-194, 1970.

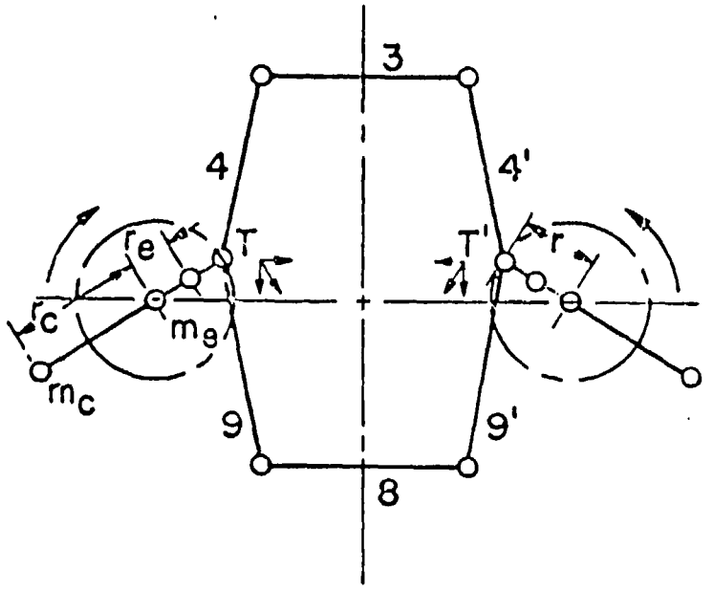

Figure 3: Conventional rhombic drive configuration

By symmetry, it can be seen that the sum of all inertial forces acting horizontally is zero at any given instant. The same applies to all inertial-force moments about an axis perpendicular to the plane of the drawing. Hence, only the inertial forces acting in the vertical direction need be considered. The circular motion of each crankpin T-T' can be resolved into a vertical and horizontal component. The vertical movements that the piston and displacer make as a result of the horizontal movement of the crankpins are equal and opposite because the connecting rods are of equal length (i.e., symmetrical deformation of the "rhombus"). Thus, if the masses of the piston and displacer (including their respective rods, etc.) are made equal, i.e.,

$$m_p = m_d$$

then the sum of the vertical inertial forces corresponding to horizontal crankpin movement is always zero.

There remains the vertical movements of piston and displacer as a result of the vertical component of the crankpin movement. These movements are exactly equal and, moreover, identical with the vertical movement of the crankpins. One can therefore imagine the moving mass of the piston and displacer, $m_p + m_d$, as localized in the crankpins, $(1/2)(m_p + m_d)$ in each. By means of two counterweights m_c mounted opposite each crankpin at a suitable radius r_c, vertical inertial forces can be created which exactly balance those of $m_p + m_d$. This is true even if the rotation of the crankshafts is not exactly uniform.

In fact, the mass and offset of each counterweight are chosen such that the latter also serves to balance the crank and other eccentrically positioned moving parts. If m_e is the effective mass of all these parts, and r_e the distance of their center of gravity from the crankshaft axis, we have the following conditions for balancing:

$$r_c m_c = (1/2) r (m_p + m_d) + r_e m_e$$

From the foregoing it can be seen that the reason why it is possible to balance the inertial forces in this type of mechanism is that there are two reciprocating masses whose movements differ in phase. The configuration lends itself to the use of two motors (one on each shaft) running in opposite directions; as a result it is possible to balance the reaction torques on the motor housings as well.

Appendix D

OPERATING INSTRUCTIONS FOR AEROFLEX MOTORS

1. INTRODUCTION

The Aeroflex motors are brushless d.c. motors utilizing light emitting diodes (LED's) for switching. These motors are aligned and ready for operation.

2. PARTS

- Two rotors and stators
- Electronic controller
- Three cables: P_1, P_2, P_3. P_1 is for the 24 Vdc power leads (+) red, (-) black; P_2 is for the sensor disk and LED electronics; P_3 is for the motor winding leads.
- Glass encoder disk and its support fixture
- Three LED's and support ring.

3. SETUP PROCEDURE

3.1 Connecting Controller to 24 Vdc

Preset power supply to 24 Vdc ± 1 V to avoid excessive voltage spikes. Voltages greater than 40 Vdc or current greater than 8 A will damage the electronics. To avoid this, an ON-OFF switch is supplied with a conservatively rated fuse in the circuit.

The power supply is connected to the controller via a cable to P_1 with (+) red and (-) black. Turn switch on and the unit is ready for testing.

3.2 Motor Alignment

If for any reason the rotors or stators are disassembled or if the glass encoder disk is removed or shifted relative to its shaft, the motor will have to be realigned.

3.2.1 Procedure for Aligning Motors

(a) Preset power supply to 24 Vdc as in Paragraph 3.1.

(b) Note wiring diagram and mark each wire according to the diagram, so that it can be identified after it is unsoldered.

(c) Disconnect all the wires from the feed-through plug (for convenience in aligning the motors) and attach all the wires from P_3 (eight wires) to a terminal strip. Also attach all the wires from the P_2 plug (except N) to another terminal strip.

(d) Connect the front motor (motor with glass encoder disk & sensors) to P_3 terminal strip following color code from wiring diagram.

(e) Connect the wires from the sensor disk (five wires) to the other terminal strip P_2, following wiring diagram. For now, leave red wire C from P_2, disconnected.

(f) Keep all other loose wires away from each other to prevent shorts.

(g) Turn the ON-OFF switch to the ON position for a short time (approximately 2 seconds) and then turn off and note if the rotors have turned. If they did, note which direction (c.w. or c.c.w.) and how much current was drawn. When the motor is set up properly, it should draw about 1 A. If the rotors do not turn or if they turn in a c.w. direction or if more than 1 A is drawn, then the motors are not operating properly.

(h) Loosen the three screws that secure the glass encoder disk and rotate the disk about 10° in either direction, keeping the motor shafts stationary. Tighten the three screws again. Turn the ON-OFF switch ON and again note rotor direction and amount of current drawn. By this process of rotating the glass encoder disk to a certain position relative to the shaft, one is aligning the LED's and in essence triggering the electronic logic and determining when and which motor windings are being energized and for what period of time.

Eventually one will find a correct position for the glass encoder disk that will give a c.c.w. direction with a current of approximately 1 A or less. Before proceeding to the next step, be sure the three screws that hold the encoder disk in place are tight, so that the disk is fixed to the shaft.

3.2.2 Fine Adjustment Using the Two LED's

(a) Turn the ON-OFF switch to ON position and note the current drain on the ammeter.

(b) Using a screw driver, loosen the two screws on both sides of one of the LED's and while the motors are running, move the loose LED circumferentially until reaching the lowest current reading on the ammeter. Lock the LED in place and go through the same procedure for the other LED.

By moving the LED's one is actually making a fine adjustment of what was just previously done with the glass encoder disk. These LED's are to be set so that a minimum amount of current is drawn.

3.2.3 Alignment of Rotor and Stator

(a) The motors must be phased in together because only one sensor is being used for both motors. The procedure for doing this is as follows:

- Remove from terminal strip P_3, the red and brown wire from the front motor (i.e., the one with glass disk). Also take the red and brown wire from the rear motor. Connect these wires to a dual trace differential amplifier, red (-) and brown (+). Display one set of windings on one channel and the other on another channel. Turn the ON-OFF switch to the ON position and display the two traces on the scope. There should be two sinusoidal traces. If the trace is not clear, ground the shields to K on P_2. Triggering should be off one channel of the scope and both sinusoidal curves should be brought into phase with each other; in effect the two motors will be operating as one. This is done by loosening the support bracket on the back motor and rotating its stator while the motor is running. By rotating the stator and watching its display on the scope, one can phase in one displ... over the other. Once phased in, retighten the support bracket so the stator does not shift out of alignment.

3.2.4 Wiring the Back Motor

Once the two motors are in phase, they in effect are acting as one. Reattach the red and brown wire from the front motor to P_3 as it was before. The back motor is wired as the wiring diagram indicates when both motors are resoldered together and the sensor wires are also connected. The unit

should consume approximately 1 A. The last wire to connect is the red wire C from P_2; this is the speed control wire. A better trace is obtained on the oscilloscope when the C wire is left unattached during the alignment procedure.

If the unit consumes more than 1 A after the second motor is connected, recheck the alignment of the rotor and stator, and if necessary repeat the procedure of Paragraph 3.2.3.

Finally, resolder all wires to the feed-through plug on the crankcase cover plate, following the wiring diagram. The unit is now ready for testing.

4. CAUTIONS

(a) Avoid excessive voltage (over 24 Vdc ± 1) or excessive current (over 8 A) to the motors.

(b) Do not remove the rotors from their stators. If necessary, a keeper must be used to prevent demagnetization of the motors.

WIRING DIAGRAM FOR AEROFLEX MOTORS (POWER PLUGS P_2 AND P_3)

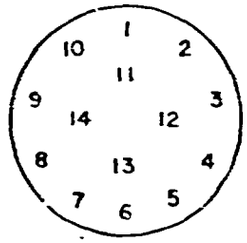

(INSIDE CRANKCASE COVER)

	PLUG	COLOR AND/OR LETTER
1.	P_3	BLUE, BLUE
2.	P_2	BLUE, E
3.	P_2	GRAY, K
4.	P_3	BROWN, BROWN
5.	P_3	VIOLET, VIOLET
6.	P_3	YELLOW, YELLOW
7.	P_3	ORANGE, ORANGE
8.	P_3	GRAY, GRAY
9.	P_3	RED, RED
10.	P_3	GREEN, GREEN
11.	P_2	BLUE, G
12.	P_2	RED, J
13.	P_2	C
14.	BLANK	

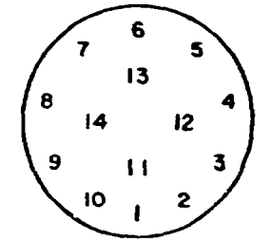

(OUTSIDE CRANKCASE COVER)

	PLUG	COLOR AND/OR LETTER
1.	P_3	YELLOW
2.	P_2	ORANGE, E
3.	P_2	BLUE, K
4.	P_3	BLACK
5.	P_3	BLUE
6.	P_3	RED
7.	P_3	ORANGE
8.	P_3	VIOLET
9.	P_3	BROWN
10.	P_3	GREEN
11.	P_2	YELLOW, G
12.	P_2	GREEN, J
13.	P_2	RED, C
14.	BLANK	